

Mechanism of Cellular Production and in Vivo Seeding Effects of Hexameric β -Amyloid Assemblies

Céline Vrancx

Université catholique de Louvain

Devkee M Vadukul

Université catholique de Louvain: Université Catholique de Louvain

Sabrina Contino

Université catholique de Louvain

Nuria Suelves

Université catholique de Louvain

Ludovic D'Auria

Université catholique de Louvain: Université Catholique de Louvain

Florian Perrin

Université catholique de Louvain: Université Catholique de Louvain

Vincent van Pesch

Université catholique de Louvain: Université Catholique de Louvain

Bernard Hanseeuw

Université catholique de Louvain

Loïc Quinton

Université de Liège

Pascal Kienlen-Campard (✉ pascal.kienlen-campard@uclouvain.be)

Université catholique de Louvain <https://orcid.org/0000-0003-1086-2942>

Research article

Keywords: Alzheimer's disease, amyloid pathology, A β oligomers, hexameric A β , seeding, 5xFAD model, CRISPR-Cas9, presenilins

Posted Date: January 8th, 2021

DOI: <https://doi.org/10.21203/rs.3.rs-138906/v1>

License:  This work is licensed under a Creative Commons Attribution 4.0 International License.

[Read Full License](#)

Abstract

Background

The β -amyloid peptide ($A\beta$) plays a key role in Alzheimer's disease. After its production by catabolism of the amyloid precursor protein (APP) through the action of presenilin 1 (PS1)- or presenilin 2 (PS2)-dependent γ -secretases, monomeric $A\beta$ can assemble in oligomers. In a pathological context, this eventually leads to the formation of fibrils, which deposit in senile plaques. Many studies suggest that $A\beta$ toxicity is related to its soluble oligomeric intermediates. Among these, our interest focuses on hexameric $A\beta$, which acts as a nucleus for $A\beta$ self-assembly.

Methods

Biochemical analyses were used to identify hexameric $A\beta$ in a wide range of models; cell lines, cerebrospinal fluid from cognitively impaired patients and transgenic mice exhibiting human $A\beta$ pathology (5xFAD). We isolated this assembly and assessed both its effect on primary neuron viability *in vitro*, and its contribution to amyloid deposition *in vivo* following intracerebral injection. In both cases, we used wild-type mice (C57BL/6) to mimic an environment where hexameric $A\beta$ is present alone and 5xFAD mice to incubate hexameric $A\beta$ in a context where human $A\beta$ species are pre-existing. Using CRISPR-Cas9, we produced stable *knockdown* human cell lines for either PS1 or PS2 to elucidate their contribution to the formation of hexameric $A\beta$.

Results

In WT mice, we found that neither *in vitro* or *in vivo* exposure to hexameric $A\beta$ was sufficient to induce cytotoxic effects or amyloid deposition. In 5xFAD mice, we observed a significant increase in neuronal death *in vitro* following exposure to $5\mu\text{M}$ hexameric $A\beta$, as well as a 1.47-fold aggravation of amyloid deposition *in vivo*. At the cellular level, we found hexameric $A\beta$ in extracellular vesicles and observed a strong decrease in its excretion when PS2 was knocked down by 60%.

Conclusions

Our results indicate the absence of cytotoxic effects of cell-derived hexameric $A\beta$ by itself, but its capacity to aggravate amyloid deposition by seeding other $A\beta$ species. We propose an important role for PS2 in the formation of this particular assembly in vesicular entities, in line with previous reports linking the restricted location of PS2 in acidic compartments to the production of more aggregation-prone $A\beta$.

Background

The β -amyloid peptide ($A\beta$) is the major constituent of the senile plaques, a typical histological hallmark of Alzheimer's disease (AD). This peptide is produced by the amyloidogenic catabolism of the amyloid precursor protein (APP) [1]. APP undergoes a first cleavage by β -secretase, producing a C-terminal fragment (βCTF), which in turn is cleaved by γ -secretase to generate the intracellular domain of APP

(AICD) and A β . To note, different isoforms of A β are produced, mostly ranging from 38 to 43 amino acids [2]. After its release as a monomer, A β , particularly in its longer forms (A β_{42} , A β_{43}), is very prone to self-assembly. In AD, this ultimately leads to the formation of amyloid fibrils, aggregating into senile plaques in the brain. Many studies suggest that the toxicity of A β does not lie in these insoluble fibrils but rather in its soluble oligomeric intermediates, as a result of their intrinsically misfolded nature and aggregation propensity that might contribute to trapping vital proteins or cause cell membrane alterations [3, 4]. Further, A β has been reported to have seeding properties. A particular study showed that A β -rich brain extracts are capable of inducing cerebral amyloidosis when inoculated into APP transgenic mice, but not into APP *knockout* mice. However, brain extracts from these previously inoculated APP *knockout* mice, that themselves do not bear amyloidosis, were still capable of inducing amyloidosis when in turn inoculated into APP transgenic mice [5]. This model of secondary transmission reveals the potential of A β to stably persist in the brain and also to retain pathogenic activity by acting as seeds when in the presence of host A β that can be propagated. Hence, it is believed that the stability of A β , and particularly A β oligomers, gives them persistent and aggravating pathological properties for the formation of amyloid deposits [6].

A β assembly is thought to rely on a process of nucleated polymerization [7–9], involving a nucleation phase during which unfolded or partially folded A β monomers self-associate to form an oligomeric nucleus. This will give rise to protofibrils through further elongation, and eventually to mature amyloid fibrils. Many A β assemblies have been identified as important intermediates of this pathway converting A β monomers into amyloid fibrils. The so-called on-pathway assemblies range from low-molecular-weight oligomers including dimers, trimers, tetramers and pentamers, to midrange-molecular-weight oligomers including hexamers, nonamers and dodecamers [10–14]. In addition, globular non-fibril forming A β aggregates have also been identified and labelled as off-pathway assemblies [15]. These include annulus and amylospheroid structures as well as dodecameric A β -derived diffusible ligands (ADDLs).

Many oligomeric structures seem to play an important role in A β assembly and to have deleterious effects that could explain A β -related toxicity [10, 16–21]. Among these assemblies, A β hexamers currently gain increasing interest. Indeed, they have recently been identified, together with pentamers, as the smallest oligomeric species that A β_{42} forms in solution [22]. Other studies based on mass spectrometry reported these assemblies as the previously mentioned nucleus (also termed “paranucleus”) that can serve as a building block for the elongation step of A β assembly [15, 23, 24]. This idea is supported by the fact that at least four other A β species are comprised of multiples of this basic hexameric unit [15, 17, 25, 26].

Altogether, these findings prompt a more in-depth understanding of the role of the different A β assemblies in fibrillation and deposition, but also in unravelling their intrinsic toxic properties, particularly in the case of the potentially nucleating hexamers discussed above. In this context, we previously reported the presence of ~ 28 kDa oligomeric assemblies in cell lysates and culture media of CHO (Chinese hamster ovary) cells expressing amyloidogenic fragments of human APP [27]. The data

reported herein demonstrate that these assemblies likely correspond to A β ₄₂ hexamers. Importantly, we identified hexameric A β assemblies across several cell lines, as well as in a well-established mouse model of amyloid pathology (5xFAD [28]) and in the cerebrospinal fluid (CSF) of cognitively impaired patients. We isolated hexameric A β from CHO cells and assessed its cytotoxic potential *in vitro* on primary neurons, as well as its potential to drive amyloid deposition *in vivo* following intracerebral stereotaxic injection. Very recent biochemical studies from our group revealed the ability of cell-derived hexameric A β to enhance the aggregation of synthetic A β monomers [29]. To address the pathological properties of hexameric A β in the brain, we used two mouse models: WT mice (C57BL/6) to measure the ability of the hexamers to form amyloid deposits in a non-pathological context, and transgenic 5xFAD mice to study their effect on the spreading of amyloid pathology. We found that cell-derived hexameric A β is a stable assembly that does not induce toxic effects by itself, but nucleates A β assembly in a pathological context where human A β accumulates (5xFAD).

As mentioned above, the production of A β relies on the cleavage of the β CTF membrane fragment of APP by the γ -secretase complex [1]. The catalytic core of γ -secretase is formed by either presenilin 1 (PS1) or presenilin 2 (PS2) [30, 31]. A recent cryo-EM study revealed a similar structure and conformational state between both presenilins (PSs), suggesting similar catalytic activities, but differences in their membrane-anchoring motifs [32]. We and others have repeatedly shown a major contribution of PS1 to A β production intended as substrate cleavage [33–37], rendering the exact role of PS2 in the amyloid pathology less understood, and in turn PS2 less attractive as a therapeutic target. However, more recent findings revealed the enrichment of PS2 γ -secretases in endosomal compartments, which might explain its lesser overall contribution to substrate cleavage simply by secondary encounters; substrates such as APP and its CTFs are indeed likely to be efficiently processed in cells first along trafficking through the secretory pathway and at the plasma membrane before reaching the endosomal pathway [38]. Further, PS2-dependent γ -secretases were shown to produce the intracellular pool of A β , in which longer forms prone to aggregation are accumulating [39]. Interestingly, extracellular vesicles (EVs), which are enclosed lipid membrane entities stemmed from cells circulating in biological fluids, are increasingly referred to as mediators of AD pathogenesis [40]. EVs could thus be involved in the extracellular release of specific A β assemblies and resulting seeding.

Together, these observations indicate that understanding the respective contribution of PS1- and PS2-dependent γ -secretases and related cellular pathways in the production of A β species that underpin the pathological processes at stake is of critical importance. In this context, we developed a model of stable human neuroblastoma-derived SH-SY5Y cell lines *knockdown* for each of the two PSs using the CRISPR-Cas9 homology-directed repair (HDR) technique [41, 42]. We assessed the profile of A β production in these cells in an effort to understand the contribution of PS1- and PS2-dependent γ -secretases in the formation of the A β hexamers discussed above. Our findings reveal a potentially important role of PS2 in the extracellular release of hexameric A β inside EVs, in agreement with the recent findings re-appraising the role of PS2 in the amyloid pathology.

Materials And Methods

Chemicals and reagents

Reagents used for Western blotting – Pierce BCA protein assay kit, SeeBlue™ Plus2 pre-stained standard, NuPAGE™ 4–12% Bis-Tris protein gels, NuPAGE™ MES SDS Running Buffer (20X), NuPAGE™ Transfer Buffer (20X), nitrocellulose 0.1 μm membranes and GE Healthcare ECL Amersham™ Hyperfilm™ – were purchased from ThermoFisher (Waltham, MA, USA). Western Lightning® Plus-ECL was from Perkin Elmer (Waltham, MA, USA). Complete™ protease inhibitor cocktail was from Roche (Basel, Switzerland). Primary antibodies targeting human Aβ; anti-Aβ clone W0-2 (MABN10), anti-Aβ₄₀ and anti-Aβ₄₂ were from Merck (Kenilworth, NJ, USA); anti-Aβ clone 6E10 (803001) was from BioLegend (San Diego, CA, USA). Primary antibody directed against the C-terminal part of APP (APP-C-ter) (A8717) was purchased from Sigma-Aldrich (St-Louis, MO, USA). Anti-PS1 (D39D1) and anti-PS2 (D30G3) antibodies were from Cell Signalling (Danvers, MA, USA). Anti-α-tubulin primary antibody as well as secondary antibodies coupled to horseradish peroxidase (HRP) were obtained from Sigma-Aldrich. AlexaFluor-labelled secondary antibodies were obtained from ThermoFisher. Thioflavin T (ThT) amyloid stain was obtained from Sigma-Aldrich. Mowiol® 4–88 used for mounting medium was purchased from Merck (Kenilworth, NJ, USA). Cell culture reagents – Ham's-F12, DMEM-F12, DMEM and Neurobasal® growth media, penicillin-streptomycin (p-s) cocktail, Lipo2000® transfection reagent, Opti-MEM®, HBSS, glutamine and B-27® – were all purchased from ThermoFisher. Fetal bovine serum (FBS) was from VWR (Radnor, PA, USA). GELFrEE™ 8100 12% Tris Acetate cartridge kits were purchased from Expedeon (Heidelberg, Germany). ReadyProbes® cell viability assay kit was from ThermoFisher. Reagents used for plate-based immuno-Europium assay were ELISA strip plate (F8, high-binding 771261) from Greiner Bio-One, reagent diluent-2 10x (DY995) from R&D systems. Anti-CD9 primary antibody (MAB1880) was from R&D systems, anti-CD81 (TAPA-1, 349502) from Biolegend, anti-CD63 (MCA2142) from Serotec Bio-Rad and anti-GM130 (610823) from BD transduction. The anti-mouse IgG-biotin (NEF8232001EA), Europium-labeled streptavidin (1244 – 360), Delfia wash concentrate 25 × (4010-0010), Delfia assay buffer (1244 – 111) and Delfia enhancement solution (1244 – 105) were all from Perkin-Elmer.

DNA constructs

The pSVK3-empty (EP), -C42 and -C99 vectors used for expression in rodent cell lines (CHO, MEF) were described previously [27, 43]. C42 and C99 are composed of the human APP signal peptide fused to the Aβ₄₂ and βCTF sequences, respectively. For expression in human cell lines (HEK293, SH-SY5Y), the C99 construct in a pCDNA3.1 plasmid was kindly provided by R. Pardossi-Piquard (University of Sophia Antipolis, Nice, France). The pCDNA3.1 plasmid bearing the C99-GVP construct used in reporter gene assays was a gift from H. Karlström (Karolinska Institute, Stockholm, Sweden). The associated Gal4RE-*Firefly* luciferase reporter gene (pG5E1B-luc) and *Renilla* luciferase reporter vector (pRL-TK) have been described previously [37, 44].

Cell lines culture and transfection

Chinese hamster ovary (CHO) cell lines were grown in Ham's F12 medium. Human neuroblastoma SH-SY5Y and mouse embryonic fibroblasts (MEF) cell lines were grown in DMEM-F12. Human embryonic kidney (HEK293) cell lines were grown in DMEM. All media were supplemented with 10% of heat-inactivated FBS and 1% of p-s solution (100units/ml final). All cell cultures were maintained at 37 °C in a humidified atmosphere and 5% CO₂.

For transient transfection, cells were seeded 24 h before transfection at a density of 40.000cells/cm². Transfection mixes containing desired DNA and Lipo2000® were prepared in Opti-MEM® and pre-incubated for 15 min at room temperature (rt) to allow for liposomal complex formation. One day after transfection, medium was changed to fresh FBS-free culture medium and incubated for another 24 h. Cell lysates and culture media were harvested 48 h after transfection for analysis.

Western blotting

Cells were rinsed and scraped in phosphate-buffered saline (PBS) and centrifuged for 5 min at 7.000 x *g*. Pellets were sonicated in lysis buffer (125 mM Tris pH 6.8, 20% glycerol, 4% SDS) with Complete™ protease inhibitor cocktail. Protein concentration was determined using the BCA protein assay kit (Pierce, Rockford, IL, USA). Fifteen (for detection with anti-PS1 or PS2 primary antibodies) or forty (for detection with anti-Aβ or APP-C-ter primary antibodies) micrograms of protein were heated for 10 min at 70 °C in loading buffer (lysis buffer containing 50 mM DTT and NuPAGE™ LDS sample buffer (ThermoFisher)). Samples were loaded and separated by SDS-PAGE electrophoresis on Nupage™ 4–12% Bis-Tris gels with MES SDS Running buffer, using SeeBlue™ Plus2 pre-stained as a protein standard. Proteins were then transferred for 2 h at 30V with NuPAGE™ transfer buffer onto 0.1μ m nitrocellulose membranes. After blocking (5% non-fat milk in PBS-Tween 0.1%), membranes were incubated overnight at 4 °C with the primary antibodies, then washed, and incubated with the secondary antibodies coupled to HRP for 1 h prior to ECL detection. Primary antibodies were used as follows: anti-human Aβ clone W0-2 (1:1.500), anti-human Aβ clone 6E10 (1:1.500), anti-APP-C-ter (1:2.000), anti-PS1 (1:1.000), anti-PS2 (1:1.000), anti-β-actin (1:3.000) or anti-α-tubulin (1:3.000). Secondary antibodies were used as follows: HRP-coupled anti-mouse IgG (1:10.000) or anti-rabbit IgG (1:10.000).

GELFrEE isolation of cell-derived hexameric Aβ

Forty-eight hours after transfection with either pSVK3-EP, -C42 or -C99, the culture media of CHO cells was collected, lyophilized, re-suspended in ultrapure water and pre-cleared with recombinant protein A sepharose (GE Healthcare, Chicago, IL, USA). Immunoprecipitation of Aβ species from the media was performed with the monoclonal anti-Aβ clone W0-2 (MABN10) antibody. Samples were separated through a Gel Eluted Liquid Fraction Entrapment Electrophoresis (GELFrEE™) 8100 system to allow the collection of the desired kDa range of proteins directly in liquid fraction. The following method was used; step 1: 60 min at 50V, step 2: 6 min at 70V, step 3: 13 min at 85V and step 4: 38 min at 85V. Fractions 1, 2 and 3 (Fig. 1) were collected in the system running buffer (1X buffer; 1% HEPES, 0.01% EDTA, 0.1% SDS and 0.1% Tris) at the end of step 2, 3 and 4 respectively. Samples were aliquoted and kept at -20 °C until use.

Dot blotting

5 μ l of isolated hexameric A β (150 μ M for isoform characterization or 15 μ M for fractions evaluation prior to intracerebral injection) and 5 μ l of 50 μ M synthetic monomeric A β ₄₀ or A β ₄₂ were spotted onto 0.1 μ m nitrocellulose membranes and allowed to dry. Another 5 μ l of sample were then spotted twice on top and dried. The membranes were boiled twice in PBS for 3 min, then blocked with 5% non-fat milk in PBS-Tween 0.1% as for Western blotting. Membranes were then washed and incubated with primary and secondary antibodies prior to ECL detection as described above. Primary antibodies dilutions were used as follows: anti-human A β clone W0-2 (1:1.500), anti-A β ₄₀ (1:1.000), anti-A β ₄₂ (1:1.000). Secondary antibodies were used as described for Western blotting.

Animal models

Transgenic 5xFAD mice (Tg6799) harboring human APP and PS1 transgenes were originally obtained from the Jackson Laboratory: B6SJL-Tg(APP^{Sw}FILon, PSEN1*^{M146L}*^{L286V})6799Vas/Mmjax (34840-JAX). Colonies of 5xFAD and non-transgenic (wild-type, WT) mice were generated from breeding pairs kindly provided by Pr. Jean-Pierre Brion (ULB, Brussels, Belgium). All mice were kept in the original C57BL/6 background strain. Animals were housed with a 12 h light/dark cycle and were given *ad libitum* access to food and water. All experiments conducted on animals were performed in compliance with protocols approved by the UCLouvain Ethical Committee for Animal Welfare (reference 2018/UCL/MD/011).

Protein extraction from mouse brain tissues

WT and 5xFAD mice were euthanized by cervical dislocation or using CO₂ and brains were quickly removed. The hippocampus as well as a portion of temporal cortex were immediately dissected on ice. Brain tissues were then homogenized by sonication in ice-cold lysis buffer (150 mM NaCl, 20 mM Tris, 1% NP40, 10% glycerol) with Complete™ protease inhibitor cocktail until homogenous. Samples were stored at -80 °C until use. Protein concentration was determined using the BCA protein assay kit prior to analysis.

Cerebrospinal fluid collection

Cerebrospinal fluid (CSF) was collected by lumbar puncture from AD patients and symptomatic controls undergoing diagnostic work-up at the Cliniques Universitaires Saint-Luc (UCL, Brussels, Belgium), following the international guidelines for CSF biomarker research [45]. Collected samples were directly frozen at -80 °C until analysis and were always manipulated on ice during Western blotting and ECLIA experiments. Included patients signed an internal regulatory document, stating that residual samples used for diagnostic procedures can be used for retrospective academic studies, without any additional informed consent (ethics committee approval: 2007/10SEP/233). AD patients participated in a specific study referenced UCL-2016-121 (Eudra-CT: 2018-003473-94). In total, CSF samples from eight subjects were retrospectively monitored in this study (see Additional File 2).

Electro-chemiluminescence immunoassay (ECLIA) for monomeric A β quantification

A β monomeric peptides were quantified in CSF samples as well as in the culture media of SH-SY5Y cells using the A β multiplex ECLIA assay (Meso Scale Discovery, Gaithersburg, MD, USA) as previously described [46]. A β was quantified according to the manufacturer's instructions with the human A β specific 6E10 multiplex assay. For SH-SY5Y, cells were conditioned in FBS-free medium for 24 h and cell medium was collected, lyophilized and re-suspended in ultrapure water.

Primary neuronal cultures

Primary cultures of neurons were performed on E17 mouse embryos as described previously [47]. Briefly, cortices and hippocampi were isolated by dissection on ice-cold HBSS and meninges were removed. Tissues were then dissociated by pipetting up and down 15 times with a glass pipette in HBSS-5 mM glucose medium. Dissociation was repeated 10 times with a flame-narrowed glass pipette and allowed to sediment for 5 min. Supernatant containing isolated neurons was then settled on 4 ml FBS and centrifuged at 1.000 x *g* for 10 min. The pellet was resuspended in Neurobasal® medium enriched with 1 mM L-glutamine and 2% v/v B-27® supplement medium. Cells were plated at a density of 100.000cells/cm² in 12w plates pre-coated with poly-L-lysine (Sigma-Aldrich). Cultures were maintained at 37 °C and 5% CO₂ in a humidified atmosphere. Half of the medium was renewed every 2 days and neurons were cultured for 8 days *in vitro* (DIV8) before being used for cell viability experiments.

Cell viability assay (ReadyProbes®)

To assess the toxicity of cell-derived hexameric A β *in vitro*, primary neuronal cultures performed from WT and 5xFAD mouse embryos were incubated (at DIV7) with 1 or 5 μ M of either cell-derived hexameric A β (C42 fraction) or control (EP fraction). At DIV8, 2drops/ml of each reagent of the ReadyProbes® assay were added to cells: NucBlue® Live reagent for the staining of all nuclei and NucGreen® Dead reagent for the nuclei of cells with compromised plasma membrane integrity. Staining were detected with standards DAPI and FITC/GFP filters respectively, at an EVOS® FL Auto fluorescence microscope. Quantification was performed by counting dead vs total cells on ImageJ.

Intracerebral stereotaxic surgery

Stereotaxic injections of isolated A β hexamers were performed in WT and 5xFAD mice to analyze the effect of cell-derived β -amyloid hexamers on the development of A β pathology *in vivo*. 2-month-old mice were deeply anesthetized by intra-peritoneal injection of a mixture of ketamine (Ketamin®) (10 mg/kg) and medetomidine (Domitor®) (0.5 mg/kg) and placed in a stereotaxic apparatus (Kopf® Instruments). 2 μ l of 15 μ M cell-derived A β hexamers (C42 fraction) or control (EP fraction) were injected using a 10 μ l Hamilton syringe and an automated pump (RWD®) in the hippocampus (A/P -1.94; L +2.17; D/V -1.96; mm relative to bregma). 30 days after stereotaxic injection, mice were transcardially perfused with PBS and brains were post-fixed in 4% paraformaldehyde for 24 h at 4 °C.

Immunohistofluorescence

For immunohistological analysis, free-floating coronal sections (50 μm) were generated from agarose-embedded fixed brains using a vibrating HM650V microtome and were preserved in PBS-sodium azide 0.02% at 4 °C. Prior to immunomarking, sections were washed in PBS and subsequently blocked and permeabilized with PBS-BSA 3%-TritonX100 0.5% for 1 h at rt. Sections were then incubated with anti-human A β clone W0-2 (MABN10, 1:100) overnight at 4 °C as a marker for A β . After three PBS washes and incubation with AlexaFluor647-coupled secondary antibody (1:500) for 1 h at rt, slices were finally washed three times with PBS and mounted on SuperFrost® slides. Slides were then incubated with ThT (0.1 mg/ml in ethanol 50%) for 15 min at rt as a marker for fibrillar deposits. After three washes with ethanol 80% and a final wash with ultrapure water, coverslips were mounted with Mowiol® 4-88-glycerol. W0-2 and ThT staining were detected with FITC/Cy5 and GFP respectively at an EVOS® FL Auto fluorescence microscope. Counting of double-positive dots was performed on ImageJ.

Generation of SH-SY5Y PS1 and PS2 deficient cells by CRISPR-Cas9

To generate PS1 and PS2 deficient cells, kits each containing 2 guide RNA (gRNA) vectors that target human *PSEN1* or *PSEN2* genes, a GFP-puromycin or RFP-blasticidin donor vector respectively, and a scramble control were obtained from Origene (CAT#: KN216443 and KN202921RB). Target sequences were flanked with specific homology sequences for the stable integration of donor sequences, based on the homology-directed repair technique [41, 42]. SH-SY5Y cells were transfected using Lipo2000® according to the manufacturer's instructions (*cf.* Cell culture and transfection section). Two days after transfection, cells were FACS-sorted for GFP+ (PS1) or RFP+ (PS2) cells and seeded in 24w plates. Following a few days for cell-growth, a second selection was performed using puromycin (PS1) or blasticidin (PS2) at a concentration of 15 μ g/ml or 30 μ g/ml, respectively. Cells were allowed to grow again and split twice before sub-cloning in 96wells. Clonal populations were then assessed for PSs protein expression by Western blotting. PS1 and PS2 clonal populations were selected for following experiments on account of the highest gene-extinction efficiency. Puromycin (2.5 μ g/ml) and blasticidin (7.5 μ g/ml) were used for the maintenance of PS1 and PS2 deficient cells, respectively.

Dual luciferase assay

SH-SY5Y cells were co-transfected with Lipo2000® (*cf.* Cell culture and transfection section) in a 1:1:1 ratio with pG5E1B-luc, pRL-TK and either a pCDNA3.1-empty plasmid (EP) or the pCDNA3.1-C99-GVP, bearing a tagged C99 to quantify the release of AICD. The system setup was previously described [37, 48]. Forty-eight hours after transfection, cells were rinsed with PBS and incubated with the reporter lysis buffer (Promega, Madison, WI, USA) for 15 min at rt. *Firefly* and *Renilla* luciferase activities were measured using the Dual-Glo® Luciferase Assay System (Promega, Madison, WI, USA) on a Sirius single tube luminometer (Berthold, Bad Wildbad, Germany). Luciferase activity corrected for transfection efficiencies was calculated as the *Firefly/Renilla* ratio.

Extracellular vesicles isolation

Ultracentrifugation was performed on media from SH-SY5Y scramble and *knockdown* cells for the isolation of vesicular entities, as previously described [49]. Briefly, culture medium was collected and underwent several centrifugation steps (all at 4 °C); 300 x *g* for 10 min for the elimination of living cells, 1.000 x *g* for 10 min to discard dead cells, 10.000 x *g* for 30 min for the removal of cellular debris, and finally 100.000 x *g* for 1 h, to collect extracellular vesicles (EVs) as a pellet and soluble proteins as supernatant. Soluble proteins were precipitated by incubation with 10% v:v trichloroacetic acid (TCA) for 30 min on ice. Both EVs and soluble proteins fractions were resuspended in 500 µl of PBS for nanoparticle tracking analysis (NTA) and plate-based immuno-Europium-assay. For Western blotting, both fractions were sonicated in lysis buffer (125 mM Tris pH 6.8, 20% glycerol, 4% SDS) with Complete™ protease inhibitor cocktail. Protein concentration was determined using the BCA protein assay kit.

Nanoparticle tracking analysis (NTA)

EVs were counted in each fraction by the Zetaview (ParticleMetrix,GmbH), which captures Brownian motion through a laser scattering microscope combined with a video camera to obtain size distribution (50-1000 nm) and concentration. Samples were diluted 1:50 in PBS to reach 50–200 particles/frame, corresponding to ~ 2.10⁷–1.10⁸ particles/ml. Sensitivity was set to 65 and camera shutter to 100 in order to detect less than 3 particles/frame when BPS alone was injected, to assess background signal. Measurements were averaged from particles counted in 11 different positions for 2 repeated cycles with camera at medium resolution mode.

Plate-based Europium-immunoassay

50 µl of EVs and soluble fractions were bound to protein-binding ELISA plates. After overnight incubation at 4 °C, the rest of the experiment was performed at rt by shaking on a tilting shaker at 30 rpm. The plate was washed with Delfia buffer (diluted to 1x in PBS; Delfia-W), then blocked with reagent diluent-2 (diluted to 1% BSA in PBS) for 90 min. The bound material was labelled with primary antibodies against CD9, CD81, CD63 and GM130 (1 µg/ml in reagent diluent-2 diluted to 0.1% BSA in PBS) for 90 min. After three Delfia-W washes, goat anti-mouse biotinylated antibody (1:2.500 in reagent diluent-2 diluted to 0.1% BSA in PBS) was added for 60 min. After three Delfia-W washes, Europium-conjugated streptavidin (diluted to 1:1.000 in Delfia assay buffer assay) was added for 45 min. After six final Delfia-W washes, Delfia enhancement solution was incubated for 15 min before measurement using time-resolved fluorometry with exc/em 340/615 nm, flash energy/light exposure high/medium and integration lag/counting time 400/400µs (Victor X4 multilabel plate reader, PerkinElmer).

Statistical analyses

The number of experiments (N) and the number of samples per condition in each experiment (n) are indicated in figure legends. All statistical analyses were performed using the GraphPad Prism 8 software (GraphPad Software, La Jolla, CA, USA). Gaussian distribution was assessed using the Shapiro-Wilk test. A parametric test was applied if the data followed normal distribution. Otherwise, non-parametric tests

were used. When tested groups were each expressed as a fold-change of their corresponding control, the value of the control was set as the hypothetical value for the use of parametric one-sample *t* test or non-parametric one-sample Wilcoxon single-ranked test. When a correlation between two variables was assessed, Pearson's R correlation coefficient was calculated. When two groups were compared, parametric *t* test with Welch's correction or non-parametric Mann-Whitney test were used. When more than two groups were compared, parametric ANOVA with indicated *post hoc* tests or non-parametric Kruskal-Wallis were used. Significance is indicated as: ns = non-significant, *=*p* < 0.05, **=*p* < 0.01, ***=*p* < 0.001. Actual *p*-values of each test are indicated in the corresponding figure legend.

Results

Identification of cell-derived hexameric A β ₄₂ in CHO cells expressing human APP metabolites

Considering the emerging body of evidence pointing to the pathological properties of oligomeric A β assemblies, we first assessed the profile of A β production in a widely used cell model; the CHO (Chinese hamster ovary) cell line. We transiently transfected these cells with vectors expressing the human sequences of either A β ₄₂ or β CTF, each fused to the signal peptide of the full-length APP protein (Fig. 1A) to ensure a proper cellular trafficking of the expressed fragments. These constructs will be referred to as C42 and C99 respectively. The cell-derived A β assemblies were analyzed by Western blotting with several monoclonal antibodies targeting the human A β sequence (W0-2 and 6E10 clones) or the APP C-terminal region (APP-C-ter). Strikingly, we reproducibly detected a band at ~ 28 kDa in both C42 and C99 conditions with A β -specific antibodies (W0-2 clone in Fig. 1B and 6E10 clone in Additional File 1). This assembly is not recognized by the APP-C-ter specific antibody (Fig. 1B), supporting the idea that it is formed by assembly of the A β fragment, and likely corresponds to an A β ₄₂ hexamer. Importantly, we noticed a key difference between C42- and C99-expressing cells; when C42 is expressed, only the hexameric A β assembly is detected in both cell lysates and media, while in the C99 condition, which requires processing by γ -secretase to release A β , we detect several intermediate A β assemblies; monomers, dimers, trimers and hexamers (Fig. 1B). This suggests that the A β , whether directly expressed or released by processing in the cellular context, will either readily or progressively assemble into the identified hexameric assembly. In addition, as the presence of these low-molecular-weight assemblies is only observed in the media of C99-expressing cells and not inside the cells, the ranges of A β assemblies may be produced differentially or aggregate with different kinetics depending on the extra- or intracellular context in which they accumulate.

For a further characterization of the A β assembly identified in Fig. 1B, we used a Gel Elution Liquid Fraction Entrapment Electrophoresis technique (GELFrEE™ 8100) to isolate the cell-derived A β hexamers from W0-2-immunoprecipitated media of CHO cells expressing C42 or C99 (Fig. 1C). Dot blotting with primary antibodies directed against the free C-terminal end of the two major A β isoforms (A β ₄₀, A β ₄₂) was performed on the isolated ~ 28 kDa fraction and identified it as an A β ₄₂ assembly (Fig. 1D).

Synthetic preparations of monomeric A β ₄₀ and A β ₄₂ were used as positive controls. Altogether, these results converge to the identification of the assembly of interest as cell-derived hexameric A β ₄₂.

Formation of hexameric A β across a wide range of models

As A β self-assembly strongly depends on the context of its release, we sought to determine whether the assembly of interest was produced particularly by CHO cells or commonly across other models. Using the same procedure as described above, we assessed the A β profile in transiently transfected mouse embryonic fibroblasts (MEF) (Fig. 2A) as well as two human immortalized models – human embryonic kidney (HEK293) cells (Fig. 2B) and neuroblastoma-derived SH-SY5Y cells (Fig. 2C). Importantly, the ~ 28 kDa assembly was consistently detected with the W0-2 A β specific antibody and not by the APP-C-ter targeted antibody in all the tested models (Fig. 2). This indicates that A β hexamers can readily form in a cellular context and are not restricted to one cell-type, fostering its interest as a primary nucleus for A β toxicity and amyloid pathology.

We next investigated the presence of this A β assembly in mice bearing familial AD (FAD) mutations. We readily detected the ~ 28 kDa A β assembly (Fig. 3A) in brain extracts of 5xFAD mice [28]. Interestingly, the intensity of hexameric A β increases with age. More importantly, the detection of the hexameric assembly precedes that of fibrils, which are recognized as the major indicator of the development of amyloid deposits in the 5xFAD model [28, 50]. Quantitative analysis of hexamers and fibrils relative to human APP expressed in mice brains confirms the appearance of hexameric A β as an early event (Fig. 3B). To note, the assembly of interest accumulates first in the hippocampus of the mice, as early as 2-month-old, while its increase in cortical regions peaks at 3 to 6 months of age. This is in line with the staging of amyloid pathology observed in AD and again suggests hexameric A β might serve as an early indicator of pathology development, and possibly as a nucleus for further amyloid deposition.

Finally, cerebrospinal fluid (CSF) samples from cognitively affected patients (diagnosed with non-AD dementia, pre-clinical AD or symptomatic AD) were monitored with the same Western blotting approach (Fig. 3C, left panel). Only AD-related patients revealed the presence of ~ 28 kDa assemblies, undeniably placing the assembly of interest in the pathological context of AD. More detailed information on neurological examination and PET-analyses conducted on the patients are displayed in Additional File 2. The same CSF samples were used for a quantitative analysis of monomeric A β isoforms by ECLIA immunoassay and revealed an overall reduction in the A β ₄₂/A β ₄₀ ratio in AD patients (Fig. 3C, right panel). This reduction correlated with the severity of AD symptoms exerted by the patients (see raw values in Table 1), concordantly with previous reports [51]. On the contrary, relative quantification of hexameric A β levels detected by Western blotting, using soluble APP (sAPP) as an intrasubject control, revealed an increase in hexameric levels with the progression of AD (Table 1). This suggests a correlation between the reduced proportion of monomeric A β ₄₂ and its aggregation in higher assemblies, as previously suggested [52, 53], but here particularly with the hexameric assembly. More precisely, statistical analysis revealed that 48.8% of the A β ₄₂/A β ₄₀ ratio variance can be explained by the increase in hexameric A β formation.

Table 1
Inverse correlation between monomeric and hexameric A β in human CSF samples.

Inclusion n°	Classification	A β ₄₂ /A β ₄₀	Hexameric A β /sAPP
1258	Non-AD	0.069	0.079
1506		0.065	0.055
1523	Pre-clinical AD	0.052	0.075
1268		0.080	0.084
1556		0.052	0.092
1272	Symptomatic AD	0.033	0.140
1329		0.039	0.224
1633		0.032	0.143

CSF samples from eight subjects were monitored in this study: patients n°1258 and 1506 did not exert any AD-related features. Patients n°1523, 1268 and 1556 were diagnosed with pre-clinical AD and patients n°1272, 1329 and 1633 with symptomatic AD. Ratios of A β ₄₂/A β ₄₀ and of hexameric A β /soluble APP (sAPP) were obtained from ECLIA and Western blot quantifications respectively (see Fig. 3). Pearson's R correlation test: R=-0.70 (R-squared = 0,49), p = 0.05.

Cell-derived hexameric A β causes cell viability impairment only in primary neurons expressing amyloid proteins *in vitro*

Following the detection of hexameric A β in a well-described amyloid mouse model and in the CSF of cognitively impaired patients, identifying it as an important factor in the development of amyloid pathology, we sought to assess whether isolated cell-derived hexameric A β would exert any neurotoxicity. For this, we cultured primary neurons from wild-type (WT) and transgenic (5xFAD) embryos and treated them after 7 days of differentiation *in vitro* (DIV) with hexameric A β . A β hexamers were obtained by W0-2-immunoprecipitation and GELFrEE separation of C42-expressing CHO cells media as described above (Fig. 1). The corresponding GELFrEE fraction of cells expressing the empty plasmid (EP) were used as a control. Two final concentrations were tested; 1 μ M and 5 μ M. 24 h after treatment, cell viability was assessed using a ReadyProbes® assay and a percentage of dead cells out of the total cells was quantified (Fig. 4A). Results show an absence of any significant cytotoxic effect at tested concentrations on primary neurons cultured from WT mice (Fig. 4B), even though both are above the reported neurotoxic concentrations from synthetic preparations of oligomeric A β [6, 54]. This suggests that the identified assembly is not cytotoxic by itself, at least in these experimental conditions. However, primary neurons cultured from 5xFAD mice, which can serve as an amyloid model *in vitro* [55–57], displayed increased cell death when exposed to 5 μ M of cell-derived hexameric A β . Importantly, this indicates that A β hexamers may have the ability to cause toxic effects only when there is pre-existing A β in the neuronal environment. This therefore implies that such a cytotoxic ability requires the intermediate seeding of other A β present.

Cell-derived hexameric A β aggravates *in vivo* amyloid deposition in a transgenic mouse model

To further assess its potential to drive amyloid formation, we performed hippocampal stereotaxic injections of cell-derived hexameric A β in two mouse models: (i) WT mice (C57BL/6) to assess the potential of A β hexamers to form amyloid deposits in a previously amyloid-free context, (ii) mice developing amyloid pathology (5xFAD) to mimic a situation where the hexamers are incubated with pre-existing A β , to serve as seeds and thus study whether they have a nucleating potential *in vivo*, driving the assembly and deposition of A β produced in the brain. Experimental workflow is represented in Fig. 5A. As for *in vitro* toxicity assays, A β hexamers were obtained by W0-2-immunoprecipitation and GELFrEE separation of C42-expressing CHO cells media and the corresponding fraction of EP-expressing CHO cells media was used as a control. The fraction of cell-derived hexameric A β was diluted from 150 μ M to 15 μ M prior to intracerebral injection. The control fraction was diluted in a similar manner. Specific detection of diluted cell-derived hexameric A β was confirmed by dot blotting with the W0-2 antibody (Fig. 5A, left panel). 2-month-old WT or 5xFAD mice were injected in the hippocampus of the left and right hemisphere with 2 μ l of EP (control) and C42 (cell-derived hexameric A β) diluted fractions, respectively. To evaluate A β deposition, mice were sacrificed 30 days after stereotaxic injection and coronal sections of fixed brains were co-stained with the human specific W0-2 antibody for A β and the ThT dye for fibrillar aggregates. Quantitative analysis of A β deposition was performed by counting double-positive dots (as indicated in Fig. 5A). The results showed that cell-derived hexameric A β does not have the ability to form fibrillar deposits by itself in a WT brain (Fig. 5B), but is capable of enhancing the deposition of A β present in the 5xFAD brain (Fig. 5C). In transgenic mice, the overall deposition of A β in the hemisphere injected with cell-derived hexameric A β showed a significant 1.47-fold increase when compared to the control-injected hemisphere (average (\pm SEM) of 32.39 (\pm 3.49) and 47.50 (\pm 4.74) deposits per field in control- and hexamer-injected hemispheres, respectively). Deposits were further investigated in the two regions mainly affected by amyloid pathology in AD: the hippocampus and the cortical areas (Fig. 5C). As expected, the highest increase in A β deposition was observed in the hippocampal region, where stereotaxic injections were performed (2.90-fold increase relative to control). However, levels of A β deposits were also significantly increased by a 1.74-fold in the cortex. This suggests that the injected cell-derived hexameric A β is able to propagate from the hippocampal formation to associated cortical regions to promote amyloidosis.

Insight into the cellular pathways and contribution of presenilins to the formation of cell-derived hexameric A β

Together, our results support that the identified cell-derived hexameric A β assembly has nucleating and seeding properties in the amyloid pathology. We aimed at understanding the cellular context in which this specific assembly is formed, and more precisely the contribution of PS1- and PS2-dependent γ -secretases to the formation of these pathological A β assemblies. Previous studies demonstrated that PS1 and PS2 have differential substrate specificities [32, 37] and that several factors, including their specific subcellular localization [39], can orientate their amyloidogenic processing activity to the production of more or less aggregation-prone A β isoforms.

Hence, we investigated the formation of the assembly of interest in C99-expressing cells lacking PS1 or PS2. In order to use a homogenous system and evaluate processing of the human C99 substrate by human γ -secretases, we developed stable PS1 and PS2 *knockdown* (KD) neuron-derived cell lines (SH-SY5Y cells). SH-SY5Y readily produced the hexameric A β assembly in our conditions (Fig. 2C). Cells were transfected with a CRISPR-Cas9 expression system targeting either *PSEN1* or *PSEN2* genes, and selected using fluorescent (FACS) and antibiotic resistance double-selections. Scrambled (S) target sequences for both the *PSEN1* and *PSEN2* genes were used for the development of control cell lines. After sub-cloning, the expression of both PSs was verified by Western blotting (Fig. 6A) which showed a 44.7% and 63.2% reduction of PS1 and PS2 protein levels respectively. We first assessed the ability of the KD cells to perform the initial cleavage of the C99 substrate at the ϵ -site, releasing APP intracellular domain (AICD). The AICD release from a tagged C99-GVP substrate was measured by a Gal4 reporter gene assay, as described previously [37, 48]. Results revealed an efficient cleavage of the construct in both the PS1-KD and PS2-KD cells, when compared to PS1-S and PS2-S respectively, suggesting that neither of the *knockdown* performed here affect the ability to ensure substrate cleavage. We investigated the profile of A β production in these cell lines by Western blotting. Results indicated that the reduction in PS1 levels had no significant effect on the profile of A β produced inside or outside of the cell (Fig. 6B), with no significant decrease in monomeric A β_{40} or A β_{42} measured in culture media. This is quite an unexpected observation, that could be explained by the observation that only around 50% of PS1 *knockdown* could be achieved in our model. The remaining PS1-dependent γ -secretase activity could be sufficient to efficiently process APP-derived substrates. However, while the formation of intracellular hexameric A β was similar between PS2-KD and corresponding control cells, detection of intracellular monomeric A β was lost when PS2 expression was reduced. Concomitantly, the extracellular A β assembly profile was altered in PS2-KD cells, with an increase in monomeric form (observed both by Western blotting and ECLIA) and an acute decrease in hexameric A β , suggesting that the extracellular release of hexameric A β is dependent on the presence of PS2 (Fig. 6C). This would illustrate that the absence of PS2 favors the accumulation of monomeric extracellular A β , but leads to decreased intracellular A β forms and extracellular aggregates. In other words, PS2-dependent γ -secretases could generate aggregation-prone intracellular A β , that is eventually released as an aggregate in the extracellular space. To note, PS2 [32, 39], as well as APP and intermediate fragments of its metabolism [58, 59], were previously found in endolysosomal compartments and extracellular vesicles (EVs). We examined whether hexameric A β assemblies found outside the cells were disposed of through EVs release, stemming from intracellular vesicular compartments. To discriminate whether A β species present in the media were compartmentalized in EVs, we performed a specific ultracentrifugation procedure to separate EVs from soluble proteins in the media of PS1-S, PS1-KD, PS2-S and PS2-KD cells. The efficiency of the separation was confirmed by the Europium-immunoassay with, in the EVs, significantly increased levels of inclusions markers CD9, CD63 and CD81 and lower content of the exclusion marker GM130 (Fig. 7A, left panel). The specific enrichment of inclusion markers due to higher protein content in EVs was ruled out since whole-protein assay showed larger protein amounts in soluble than EVs fractions (Fig. 7A, right panel). Finally, EVs size distribution was similar between all conditions but the number of EVs was higher in PS1-KD and PS2-KD as compared to PS1-S and PS2-S, although not significant except for PS2-S (EP)

vs PS2-KD (EP) (Fig. 7B). Importantly, extracellular monomeric A β was found exclusively in the soluble proteins fraction while hexameric A β was confined exclusively in vesicles (Fig. 7C), as was very recently reported with A β oligomeric species [49]. C99 was decreased and hexameric A β assembly almost disappeared in PS2-KD EVs, indicating that PS2 plays a critical role in the extracellular release of this specific A β assembly that displays seeding properties.

Discussion

The identification of fibrillar A β as the main component of amyloid plaques present in AD has led to the extensive investigation of the A β self-assembly process and, as a result, to the identification of many intermediate oligomeric assemblies of A β . Today, it is widely agreed that such non-fibrillar soluble assemblies exert a widespread neurotoxic effect and should be the main target of therapeutic prevention or intervention. Among A β oligomers, hexameric A β has repeatedly been identified as a key assembly *in vitro* [15, 22, 60, 61]. Our study shows the identification of a specific ~ 28 kDa assembly in a wide range of models. Using CHO cells, we were able to confirm the nature of this assembly as hexameric A β_{42} . As mentioned previously, many studies, most of which were performed on synthetic preparations of A β , have shed light on the importance of hexameric A β as a crucial nucleating step in the process of A β self-assembly [15, 23, 24, 62]. However, such studies placing hexameric A β at the core of amyloid pathology have, to the best of our knowledge, not been able to characterize the production of A β hexamers in a cellular environment, or to assess its toxic potential and relevance to AD pathogenesis.

Here, we report for the first time the identification of hexameric A β assemblies in brain extracts from a well-characterized amyloid mouse model (5xFAD) as well as in the CSF of AD patients. The question of whether this assembly is strictly speaking formed by six A β_{42} monomers associated together would require extensive analytical biochemistry investigation, which are of real interest, but beyond the scope of this study. Nevertheless, the A β assembly we identified and purified by GELFrEE electrophoresis (i) has an apparent molecular weight around 28 kDa, (ii) is recognized by W0-2, 6E10 and anti-A β_{42} antibodies but not by an APP-C-ter antibody and (iii) decreases upon PS2 *knockdown*. Together, this clearly indicates that the detected A β assembly contains A β_{42} and has the expected properties of a hexamer.

Our observations conclusively place the assembly of interest at the center of amyloid pathogenesis. In the 5xFAD model, the presence of hexameric A β followed a regional pattern of progression that corresponds to the neuropathological staging of human AD pathogenesis described by Braak and Braak [63]. Indeed, the ~ 28 kDa assembly was detected first in the hippocampus, as early as 2-month-old, and further spread to the cortex starting from 3 to 6-month-old. On the contrary, amyloid plaques formation in the 5xFAD mice have previously been reported to appear first in deep layers of the cortex and in the subiculum, and to later spread to the hippocampus as mice aged [28]. As the spreading properties of hexameric A β are likely to depend on the initial site where they are formed, it would be of interest to investigate the aggravation of amyloid pathology upon injection of cell-derived hexameric A β in the cortical areas. The pattern of hexameric A β detection reported here is also of particular importance considering the urgent need to identify early biomarkers in the development of A β pathology. In line with

this, the detection of the ~ 28 kDa assembly in CSF extracted from human patients diagnosed with pre-clinical AD and symptomatic AD supports its implication in the onset and development of the pathology. More importantly, its presence as a soluble entity in CSF is a strong argument to consider it as a novel detectable biomarker.

Furthermore, the isolation of hexameric A β from our CHO cell model has also allowed the characterization of its detrimental properties. The treatment of primary WT neurons with 1 μ M of cell-derived hexameric A β for 24 h did not indicate any cytotoxic effect. These experimental conditions mimic a cellular environment comparable to the early phase of oligomeric A β pathology, as reported in several studies [64–67]. Still, as concentrations of oligomeric A β_{42} have been reported to reach concentrations of up to 3 μ M inside AD-affected neurons [68], we also tested a 5 μ M concentration in our assay. Yet, we did not observe any increase in cell death when comparing WT neurons treated with cell-derived hexameric A β to control-treated neurons. Interestingly, another study from our group based on ThT assays and Western blotting revealed a very stable behavior of the hexameric assembly when incubated by itself *in vitro*, unable to further aggregate [29]. The lack of direct harmful effects on neurons is in line with the fact that (i) the process of A β self-assembly is thought to be vital in mediating cytotoxicity [69, 70], and that (ii) the pathological properties of A β oligomers could rely not only on their synaptotoxic effects but also on their seeding properties, propagating amyloid pathology throughout the brain parenchyma.

In line with the observation that cell-derived hexameric A β does not appear cytotoxic by itself, and considering its suggested role as a nucleus for A β self-assembly, we studied whether the harmful potential of A β hexamers could be unraveled when pre-existing A β species are present. Cytotoxic assay on primary neurons derived from transgenic 5xFAD mice was performed, as it was previously reported that cultured neurons from AD transgenic animal models can reflect AD phenotypes *in vitro* [55–57]. We observed a significant increase in the proportion of cell death when neurons were treated with 5 μ M of cell-derived hexameric A β . This suggests that this specific assembly can indeed exert a toxic effect in a FAD context, when A β to seed is likely present. To further assess this hypothesis, we performed stereotaxic injections of isolated cell-derived hexameric A β in 5xFAD mouse brains and followed A β deposition, in parallel to WT injected mice. The results obtained in WT mice suggest that the identified assembly is not able to induce A β deposition *in vivo* by itself. This is in agreement with the absence of cytotoxicity on WT primary neurons reported above. To note, A β deposition *in vivo* was assessed in a time-frame of 30 days. One cannot exclude that pathogenic mechanisms might take place upon longer incubation time. In addition, the absence of cytotoxicity or A β deposits formation by cell-derived hexameric A β *per se* does not exclude its ability to cause changes in primary neurons or in the brain function apart from toxicity or amyloid deposition. Indeed, cellular dysfunctions or alterations of neuronal connectivity might be present in our WT models and simply not yet sufficient to cause cytotoxicity or amyloidosis. Additionally, the absence of A β deposits after injection of cell-derived hexameric A β in the brain of WT mice also does not exclude the possibility that the stable seeds injected might not directly cause amyloidosis in the injected animals, but persist in the brain and retain pathogenic activity, as was previously shown with second-transmission studies [5].

A major observation in this study is the ability of cell-derived hexameric A β to act as a seeding nucleus and cause both cytotoxicity in primary neurons and aggravation of A β deposition in the brain when using transgenic 5xFAD mice. These mice express five familial AD mutations that together trigger A β ₄₂ overproduction and result in a rapid and severe development of amyloid pathology [28, 50]. 5xFAD mice therefore represented a useful model to assess the nucleating hypothesis *in vivo* in a reasonable timeframe. An earlier onset of A β aggregation in this model was previously reported upon single intracerebral injection of brain homogenates containing oligomeric A β , following a prion-like seeding mechanism [71]. A β oligomers have been further suggested as early initiating actors of the seeding process, as their depletion by passive immunization delays A β aggregation and leads to a transient reduction of seed-induced A β deposition [72]. Here, our study has the advantage of focusing on a specific cell-derived A β aggregate, that not only is an oligomeric entity of its own but also suspected, based on *in vitro* studies, to be heavily involved in the processes of nucleation and seeding [15, 29]. We chose to perform intracerebral injections at 2 months of age, when amyloid deposition begins in the 5xFAD mice [28]. The significant increase of A β deposition observed in hexamer-injected hemispheres suggests that hexameric A β is indeed able to promote amyloidosis. As very recent *in vitro* studies from our group revealed the ability of the isolated A β hexamers to drive the aggregation of synthetic monomers of A β [29], it is likely that the enhancement in A β aggregation observed here relies on the same process of nucleation, with A β hexamers serving as a template for aggregation. The greater increase of A β deposition in the hippocampus when compared to the cortex of the injected mice supports this hypothesis, as hexameric A β is likely to seed and promote A β aggregation to a higher rate at the site of injection. Still, the significant aggravation of deposition in the cortex also suggests that hexameric A β is able to spread throughout the brain, as rapidly as in 30 days. Together, these observations strongly suggest that hexameric A β accounts for a key factor in the self-assembly process, which is able to promote amyloidosis and might serve, when naturally present, as an early biomarker for A β deposition.

Following this important hypothesis, we sought to understand the cellular context in which hexameric A β is produced, in hope of unraveling potential therapeutic targets. In particular, we assessed the respective involvement of both presenilins in its production. Indeed, the distinct subcellular localizations [39] and differential substrate specificities [37] of the two types of PSs regulate the production of different A β pools. Production of A β can differ considerably between cellular compartments [39]. Pathological A β formation is related to dysfunction of the endocytic pathway, and PS1 and PS2 are differentially distributed between the secretory compartments and the late endosomes/lysosomes to which PS2 is shuttled [39]. Our results showed the absence of any significant change in the processing of C99 or the release of A β when cells have a nearly 50% reduction of PS1 protein levels. This was rather surprising regarding the previous reports on the preponderant importance of PS1 for γ -secretase substrates cleavage and overall A β production [33–37]. One can imagine, as mentioned above, that the reduction of PS1 protein levels is not significant enough to observe any effect. PS1 *knockdown* might induce compensatory mechanisms and still ensure its primary function even when its protein levels are reduced by half. In any case, results reported here bring interesting information regarding the production of hexameric A β at the cellular level. Indeed, in the PS2 *knockdown* cells, the reduction of PS2 protein levels

by just over 60% was sufficient to cause clear changes in A β production. While the initial cleavage of the C99 construct (ϵ -site) remained unaffected, the production of monomeric A β was strongly diminished inside the cell and, in an opposite manner, strongly increased in the medium. In particular, the A β_{40} isoform was increased in the extracellular medium of PS2-KD cells. Hexameric A β levels were unchanged in the cell lysates but strongly diminished in the extracellular environment. Importantly, we could discriminate for the first time that the extracellular hexameric A β was almost exclusively enriched in EVs while monomeric A β was identified solely in the soluble fraction. Notice that, although the amount of EVs tended to increase upon *knockdown* of PS1/PS2, it did not seem to impact A β fate. As PS1 and PS2 have been respectively shown to produce the extra- and intracellular pools of A β [39], the direct release of soluble A β outside the cellular environment is likely to rely mostly on the action of PS1, while the intracellular pool is likely to be mainly dependent of PS2 activity in vesicular compartments. Our observations suggest that a reduction of PS2 levels strongly influences the production of A β from the C99 fragment. Monomeric A β_{42} is likely to completely aggregate, while monomeric A β_{40} might not be able to, causing the observed increase in the detection of this isoform outside the cell. Importantly, this is supported by observations reported in a biochemical *in vitro* study [29], showing the isolation of monomeric A β from the medium of C99-expressing CHO cells and identifying it as A β_{40} , not forming any aggregates when followed over 48 h.

Together, our results in both *knockdown* cell lines drive towards the emergence of a new hypothesis according to which extracellular hexameric A β might be exclusively released in EVs emerging from the intracellular pool of A β and likely produced through the activity of PS2. The identification of such a specific role for PS2 in the release of hexameric A β that might exert nucleating effects is of particular importance. To note, PS1 and PS2 were reported to exert different sensibilities to γ -secretase inhibitors [37]. This is quite promising in the hope of re-evaluating A β modulators and developing therapeutic agents targeting a specific γ -secretase activity depending on the PS present in the complex. Importantly, the intracellular pool of A β , generated by PS2, has been repeatedly associated with the progression of AD [73–76]. FAD mutations in *PSEN2* have been shown to dramatically increase the proportion of longer length A β intracellularly, accelerating its assembly. Further, a subset of familial mutations on *PSEN1* have been reported to shift the localization of the PS1 protein to fit that of PS2 [39]. Thus, it is likely that the production of aggregation-prone A β inside intracellular compartments and its resulting accumulation and excretion are enhanced in the context of AD.

Conclusions

Altogether, our findings have shed light on a particular cell-derived A β assembly that likely corresponds to an A β_{42} hexamer. Combining *in vitro* and *in vivo* approaches, we have revealed an absence of detrimental effects of cell-derived hexameric A β by itself, but its capacity to induce cytotoxicity and aggravate amyloid deposition when there is A β to seed at disposal. An insight in cellular mechanisms at stake suggests a stronger correlation of PS2 with the formation of this particular A β oligomer, in line with

previous reports linking the restricted location of PS2 in acidic compartments to the production of more aggregation-prone A β .

Abbreviations

A β : β -amyloid. AD:Alzheimer's disease. AICD:APP intracellular domain. APP:amyloid precursor protein. CHO:Chinese hamster ovary. CRISPR:clustered regularly interspaced short palindromic repeats. Cryo-EM:cryo-electron microscopy. CSF:cerebrospinal fluid. CTF:C-terminal fragment. HEK293:human embryonic kidney. KD:*knockdown*. MCI:mild cognitive impairment. PET:positron-emission tomography. *PSEN*:presenilin (gene). PS:presenilin (protein). S:scrambled. sAPP:soluble APP. ThT:Thioflavin T. WT:wild-type.

Declarations

Ethics approval and consent to participate

All animal experiments were performed with the approval of the UCLouvain Ethical Committee for Animal Welfare (reference 2018/UCL/MD/011). Human cerebrospinal fluid samples were collected as part of clinical analyses performed at Cliniques Universitaires Saint-Luc (UCL, Brussels, Belgium). Symptomatic non-AD patients signed an internal regulatory document, stating that residual samples used for diagnostic procedures can be used for retrospective academic studies, without any additional informed consent (ethics committee approval: 2007/10SEP/233). AD patients participated to a specific study referenced UCL-2016-121 (Eudra-CT: 2018-003473-94).

Consent for publication

All authors have given consent for publication.

Availability of data and materials

All datasets generated and analyzed during this study are included in this published article and its supplementary information files. Materials are available upon request.

Competing interests

The authors declare that the research was conducted in the absence of any commercial or financial relationships that could be construed as a potential conflict of interest.

Funding

This work was supported by a grant of the Belgian F.N.R.S FRIA (Fonds National pour la Recherche Scientifique) and a grant of UCLouvain Fonds du Patrimoine to CV. Funding to PKC is acknowledged from SAO-FRA Alzheimer Research Foundation, Fondation Louvain and Queen Elisabeth Medical

Research Foundation (FMRE to PKC and LQ). The work was supported by funds from FNRS grant PDRT.0177.18 to PKC and LQ.

Authors' contributions

CV designed and performed experiments, analyzed and interpreted data, and wrote the manuscript. DMV performed experiments and analyzed data. SC and NS provided neuronal cultures and analyzed data. LD'A performed nanoparticle tracking and Europium-immunoassay analyses on isolated EVs, and helped with the analysis of related data. FP participated in experiment design and analysis. VVP and BH together provided the human CSF specimens. BH provided significant input in the interpretation of clinical data. LQ provided the GELFrEE technique and contributed to data collection. PKC designed and supervised the research project and contributed to interpretation of data. All authors revised and approved the final manuscript.

Acknowledgments

We thank Esther Paître, Sarah Houben and Pierre Burguet for technical support. We are grateful to Jean-Noël Octave, Nathalie Pierrot and Jean-Pierre Brion for providing scientific input as well as materials and animal models.

References

1. Haass C, Kaether C, Thinakaran G, Sisodia S: Trafficking and proteolytic processing of APP. *Cold Spring Harb Perspect Med* 2012, 2:a006270.
2. Takami M, Nagashima Y, Sano Y, Ishihara S, Morishima-Kawashima M, Funamoto S, Ihara Y: gamma-Secretase: successive tripeptide and tetrapeptide release from the transmembrane domain of beta-carboxyl terminal fragment. *J Neurosci* 2009, 29:13042-13052.
3. Benilova I, Karran E, De Strooper B: The toxic A β oligomer and Alzheimer's disease: an emperor in need of clothes. *Nat Neurosci* 2012, 15:349-357.
4. Almeida ZL, Brito RMM: Structure and Aggregation Mechanisms in Amyloids. *Molecules* 2020, 25.
5. Ye L, Fritschi SK, Schelle J, Obermüller U, Degenhardt K, Kaeser SA, Eisele YS, Walker LC, Baumann F, Staufenbiel M, Jucker M: Persistence of A β seeds in APP null mouse brain. *Nat Neurosci* 2015, 18:1559-1561.
6. Sengupta U, Nilson AN, Kaye R: The Role of Amyloid- β Oligomers in Toxicity, Propagation, and Immunotherapy. *EBioMedicine* 2016, 6:42-49.
7. Ferrone F: Analysis of protein aggregation kinetics. *Methods Enzymol* 1999, 309:256-274.
8. Serpell LC: Alzheimer's amyloid fibrils: structure and assembly. *Biochim Biophys Acta* 2000, 1502:16-30.
9. Fu Z, Aucoin D, Davis J, Van Nostrand WE, Smith SO: Mechanism of Nucleated Conformational Conversion of A β 42. *Biochemistry* 2015, 54:4197-4207.

10. Lambert MP, Barlow AK, Chromy BA, Edwards C, Freed R, Liosatos M, Morgan TE, Rozovsky I, Trommer B, Viola KL, et al: Diffusible, nonfibrillar ligands derived from A β 1-42 are potent central nervous system neurotoxins. *Proc Natl Acad Sci U S A* 1998, 95:6448-6453.
11. Sunde M, Blake CC: From the globular to the fibrous state: protein structure and structural conversion in amyloid formation. *Q Rev Biophys* 1998, 31:1-39.
12. Klein WL, Krafft GA, Finch CE: Targeting small A β oligomers: the solution to an Alzheimer's disease conundrum? *Trends Neurosci* 2001, 24:219-224.
13. Chen GF, Xu TH, Yan Y, Zhou YR, Jiang Y, Melcher K, Xu HE: Amyloid beta: structure, biology and structure-based therapeutic development. *Acta Pharmacol Sin* 2017, 38:1205-1235.
14. Cline EN, Bicca MA, Viola KL, Klein WL: The Amyloid- β Oligomer Hypothesis: Beginning of the Third Decade. *J Alzheimers Dis* 2018, 64:S567-s610.
15. Roychaudhuri R, Yang M, Hoshi MM, Teplow DB: Amyloid beta-protein assembly and Alzheimer disease. *J Biol Chem* 2009, 284:4749-4753.
16. Walsh DM, Klyubin I, Fadeeva JV, Rowan MJ, Selkoe DJ: Amyloid-beta oligomers: their production, toxicity and therapeutic inhibition. *Biochem Soc Trans* 2002, 30:552-557.
17. Lesné S, Koh MT, Kotilinek L, Kaye R, Glabe CG, Yang A, Gallagher M, Ashe KH: A specific amyloid-beta protein assembly in the brain impairs memory. *Nature* 2006, 440:352-357.
18. Townsend M, Shankar GM, Mehta T, Walsh DM, Selkoe DJ: Effects of secreted oligomers of amyloid beta-protein on hippocampal synaptic plasticity: a potent role for trimers. *J Physiol* 2006, 572:477-492.
19. Shankar GM, Li S, Mehta TH, Garcia-Munoz A, Shepardson NE, Smith I, Brett FM, Farrell MA, Rowan MJ, Lemere CA, et al: Amyloid-beta protein dimers isolated directly from Alzheimer's brains impair synaptic plasticity and memory. *Nat Med* 2008, 14:837-842.
20. Lesné SE, Sherman MA, Grant M, Kuskowski M, Schneider JA, Bennett DA, Ashe KH: Brain amyloid- β oligomers in ageing and Alzheimer's disease. *Brain* 2013, 136:1383-1398.
21. Müller-Schiffmann A, Herring A, Abdel-Hafiz L, Chepkova AN, Schäble S, Wedel D, Horn AH, Sticht H, de Souza Silva MA, Gottmann K, et al: Amyloid- β dimers in the absence of plaque pathology impair learning and synaptic plasticity. *Brain* 2016, 139:509-525.
22. Wolff M, Zhang-Haagen B, Decker C, Barz B, Schneider M, Biehl R, Radulescu A, Strodel B, Willbold D, Nagel-Steger L: A β 42 pentamers/hexamers are the smallest detectable oligomers in solution. *Sci Rep* 2017, 7:2493.
23. Cernescu M, Stark T, Kalden E, Kurz C, Leuner K, Deller T, Göbel M, Eckert GP, Brutschy B: Laser-induced liquid bead ion desorption mass spectrometry: an approach to precisely monitor the oligomerization of the β -amyloid peptide. *Anal Chem* 2012, 84:5276-5284.
24. Österlund N, Moons R, Ilag LL, Sobott F, Gräslund A: Native Ion Mobility-Mass Spectrometry Reveals the Formation of β -Barrel Shaped Amyloid- β Hexamers in a Membrane-Mimicking Environment. *J Am Chem Soc* 2019, 141:10440-10450.

25. Deshpande A, Mina E, Glabe C, Busciglio J: Different conformations of amyloid beta induce neurotoxicity by distinct mechanisms in human cortical neurons. *J Neurosci* 2006, 26:6011-6018.
26. Gellermann GP, Byrnes H, Striebinger A, Ullrich K, Mueller R, Hillen H, Barghorn S: Abeta-globulomers are formed independently of the fibril pathway. *Neurobiol Dis* 2008, 30:212-220.
27. Decock M, Stanga S, Octave JN, Dewachter I, Smith SO, Constantinescu SN, Kienlen-Campard P: Glycines from the APP GXXXG/GXXXA Transmembrane Motifs Promote Formation of Pathogenic A β Oligomers in Cells. *Front Aging Neurosci* 2016, 8:107.
28. Oakley H, Cole SL, Logan S, Maus E, Shao P, Craft J, Guillozet-Bongaarts A, Ohno M, Disterhoft J, Van Eldik L, et al: Intraneuronal beta-amyloid aggregates, neurodegeneration, and neuron loss in transgenic mice with five familial Alzheimer's disease mutations: potential factors in amyloid plaque formation. *J Neurosci* 2006, 26:10129-10140.
29. Vadukul DM, Vrancx C, Burguet P, Contino S, Suelves N, Serpell LC, Quinton L, Kienlen-Campard P: Cell-derived hexameric β -amyloid: a novel insight into composition, self-assembly and nucleating properties. Submitted bioRxiv doi: 101101/20201215422916 2020.
30. De Strooper B: Aph-1, Pen-2, and Nicastrin with Presenilin generate an active gamma-Secretase complex. *Neuron* 2003, 38:9-12.
31. Sato T, Diehl TS, Narayanan S, Funamoto S, Ihara Y, De Strooper B, Steiner H, Haass C, Wolfe MS: Active gamma-secretase complexes contain only one of each component. *J Biol Chem* 2007, 282:33985-33993.
32. Dehury B, Tang N, Blundell TL, Kepp KP: Structure and dynamics of γ -secretase with presenilin 2 compared to presenilin 1. *RSC Advances* 2019, 9:20901-20916.
33. De Strooper B, Saftig P, Craessaerts K, Vanderstichele H, Guhde G, Annaert W, Von Figura K, Van Leuven F: Deficiency of presenilin-1 inhibits the normal cleavage of amyloid precursor protein. *Nature* 1998, 391:387-390.
34. Frånberg J, Svensson AI, Winblad B, Karlström H, Frykman S: Minor contribution of presenilin 2 for γ -secretase activity in mouse embryonic fibroblasts and adult mouse brain. *Biochem Biophys Res Commun* 2011, 404:564-568.
35. Pintchovski SA, Schenk DB, Basi GS: Evidence that enzyme processivity mediates differential A β production by PS1 and PS2. *Curr Alzheimer Res* 2013, 10:4-10.
36. Xia D, Watanabe H, Wu B, Lee SH, Li Y, Tsvetkov E, Bolshakov VY, Shen J, Kelleher RJ, 3rd: Presenilin-1 knockin mice reveal loss-of-function mechanism for familial Alzheimer's disease. *Neuron* 2015, 85:967-981.
37. Stanga S, Vrancx C, Tasiaux B, Marinangeli C, Karlström H, Kienlen-Campard P: Specificity of presenilin-1- and presenilin-2-dependent γ -secretases towards substrate processing. *J Cell Mol Med* 2018, 22:823-833.
38. Meckler X, Checler F: Presenilin 1 and Presenilin 2 Target γ -Secretase Complexes to Distinct Cellular Compartments. *J Biol Chem* 2016, 291:12821-12837.

39. Sannerud R, Esselens C, Ejsmont P, Mattera R, Rochin L, Tharkeshwar AK, De Baets G, De Wever V, Habets R, Baert V, et al: Restricted Location of PSEN2/ γ -Secretase Determines Substrate Specificity and Generates an Intracellular A β Pool. *Cell* 2016, 166:193-208.
40. Lee S, Mankhong S, Kang JH: Extracellular Vesicle as a Source of Alzheimer's Biomarkers: Opportunities and Challenges. *Int J Mol Sci* 2019, 20.
41. Wiedenheft B, Sternberg SH, Doudna JA: RNA-guided genetic silencing systems in bacteria and archaea. *Nature* 2012, 482:331-338.
42. Hsu PD, Lander ES, Zhang F: Development and applications of CRISPR-Cas9 for genome engineering. *Cell* 2014, 157:1262-1278.
43. Kienlen-Campard P, Tasiaux B, Van Hees J, Li M, Huysseune S, Sato T, Fei JZ, Aimoto S, Courtoy PJ, Smith SO, et al: Amyloidogenic processing but not amyloid precursor protein (APP) intracellular C-terminal domain production requires a precisely oriented APP dimer assembled by transmembrane GXXXG motifs. *J Biol Chem* 2008, 283:7733-7744.
44. Huysseune S, Kienlen-Campard P, Hébert S, Tasiaux B, Leroy K, Devuyst O, Brion JP, De Strooper B, Octave JN: Epigenetic control of aquaporin 1 expression by the amyloid precursor protein. *Faseb j* 2009, 23:4158-4167.
45. Teunissen CE, Petzold A, Bennett JL, Berven FS, Brundin L, Comabella M, Franciotta D, Frederiksen JL, Fleming JO, Furlan R, et al: A consensus protocol for the standardization of cerebrospinal fluid collection and biobanking. *Neurology* 2009, 73:1914-1922.
46. Hage S, Stanga S, Marinangeli C, Octave JN, Dewachter I, Quetin-Leclercq J, Kienlen-Campard P: Characterization of *Pterocarpus erinaceus* kino extract and its gamma-secretase inhibitory properties. *J Ethnopharmacol* 2015, 163:192-202.
47. Opsomer R, Contino S, Perrin F, Galdani R, Tasiaux B, Doyen P, Vergouts M, Vrancx C, Doshina A, Pierrot N, et al: Amyloid Precursor Protein (APP) Controls the Expression of the Transcriptional Activator Neuronal PAS Domain Protein 4 (NPAS4) and Synaptic GABA Release. *eNeuro* 2020, 7.
48. Karlström H, Bergman A, Lendahl U, Näslund J, Lundkvist J: A sensitive and quantitative assay for measuring cleavage of presenilin substrates. *J Biol Chem* 2002, 277:6763-6766.
49. Perrin F, Papadopoulos N, Suelves N, Opsomer R, Vadukul DM, Vrancx C, Smith SO, Vertommen D, Kienlen-Campard P, Constantinescu SN: Dimeric Transmembrane Orientations of APP/C99 Regulate γ -Secretase Processing Line Impacting Signaling and Oligomerization. *ISCIENCE* 2020.
50. Eimer WA, Vassar R: Neuron loss in the 5XFAD mouse model of Alzheimer's disease correlates with intraneuronal A β 42 accumulation and Caspase-3 activation. *Mol Neurodegener* 2013, 8:2.
51. Doecke JD, Pérez-Grijalba V, Fandos N, Fowler C, Villemagne VL, Masters CL, Pesini P, Sarasa M: Total A β (42)/A β (40) ratio in plasma predicts amyloid-PET status, independent of clinical AD diagnosis. *Neurology* 2020, 94:e1580-e1591.
52. Gravina SA, Ho L, Eckman CB, Long KE, Otvos L, Jr., Younkin LH, Suzuki N, Younkin SG: Amyloid beta protein (A beta) in Alzheimer's disease brain. Biochemical and immunocytochemical analysis with

- antibodies specific for forms ending at A beta 40 or A beta 42(43). *J Biol Chem* 1995, 270:7013-7016.
53. Jarrett JT, Berger EP, Lansbury PT, Jr.: The carboxy terminus of the beta amyloid protein is critical for the seeding of amyloid formation: implications for the pathogenesis of Alzheimer's disease. *Biochemistry* 1993, 32:4693-4697.
54. Li X, Buxbaum JN: Transthyretin and the brain re-visited: is neuronal synthesis of transthyretin protective in Alzheimer's disease? *Mol Neurodegener* 2011, 6:79.
55. Kim H, Kim B, Kim HS, Cho JY: Nicotinamide attenuates the decrease in dendritic spine density in hippocampal primary neurons from 5xFAD mice, an Alzheimer's disease animal model. *Mol Brain* 2020, 13:17.
56. Mariani MM, Malm T, Lamb R, Jay TR, Neilson L, Casali B, Medarametla L, Landreth GE: Neuronally-directed effects of RXR activation in a mouse model of Alzheimer's disease. *Sci Rep* 2017, 7:42270.
57. Noh H, Park C, Park S, Lee YS, Cho SY, Seo H: Prediction of miRNA-mRNA associations in Alzheimer's disease mice using network topology. *BMC Genomics* 2014, 15:644.
58. Lauritzen I, Pardossi-Piquard R, Bourgeois A, Pagnotta S, Biferi MG, Barkats M, Lacor P, Klein W, Bauer C, Checler F: Intraneuronal aggregation of the β -CTF fragment of APP (C99) induces A β -independent lysosomal-autophagic pathology. *Acta Neuropathol* 2016, 132:257-276.
59. Evrard C, Kienlen-Campard P, Coevoet M, Opsomer R, Tasiaux B, Melnyk P, Octave JN, Buée L, Sergeant N, Vingtdeux V: Contribution of the Endosomal-Lysosomal and Proteasomal Systems in Amyloid- β Precursor Protein Derived Fragments Processing. *Front Cell Neurosci* 2018, 12:435.
60. Bitan G, Kirkitadze MD, Lomakin A, Vollers SS, Benedek GB, Teplow DB: Amyloid beta -protein (A β) assembly: A β 40 and A β 42 oligomerize through distinct pathways. *Proc Natl Acad Sci U S A* 2003, 100:330-335.
61. Roychaudhuri R, Yang M, Deshpande A, Cole GM, Frautschy S, Lomakin A, Benedek GB, Teplow DB: C-terminal turn stability determines assembly differences between A β 40 and A β 42. *J Mol Biol* 2013, 425:292-308.
62. Lendel C, Bjerring M, Dubnovitsky A, Kelly RT, Filippov A, Antzutkin ON, Nielsen NC, Härd T: A hexameric peptide barrel as building block of amyloid- β protofibrils. *Angew Chem Int Ed Engl* 2014, 53:12756-12760.
63. Braak H, Braak E: Neuropathological staging of Alzheimer-related changes. *Acta Neuropathol* 1991, 82:239-259.
64. Nath S, Agholme L, Kurudenkandy FR, Granseth B, Marcusson J, Hallbeck M: Spreading of neurodegenerative pathology via neuron-to-neuron transmission of β -amyloid. *J Neurosci* 2012, 32:8767-8777.
65. Hallbeck M, Nath S, Marcusson J: Neuron-to-neuron transmission of neurodegenerative pathology. *Neuroscientist* 2013, 19:560-566.
66. Domert J, Rao SB, Agholme L, Brorsson AC, Marcusson J, Hallbeck M, Nath S: Spreading of amyloid- β peptides via neuritic cell-to-cell transfer is dependent on insufficient cellular clearance. *Neurobiol*

Dis 2014, 65:82-92.

67. Sackmann C, Hallbeck M: Oligomeric amyloid- β induces early and widespread changes to the proteome in human iPSC-derived neurons. *Sci Rep* 2020, 10:6538.
68. Hashimoto M, Bogdanovic N, Volkman I, Aoki M, Winblad B, Tjernberg LO: Analysis of microdissected human neurons by a sensitive ELISA reveals a correlation between elevated intracellular concentrations of Abeta42 and Alzheimer's disease neuropathology. *Acta Neuropathol* 2010, 119:543-554.
69. Marshall KE, Vadukul DM, Dahal L, Theisen A, Fowler MW, Al-Hilaly Y, Ford L, Kemenes G, Day IJ, Staras K, Serpell LC: A critical role for the self-assembly of Amyloid- β 1-42 in neurodegeneration. *Sci Rep* 2016, 6:30182.
70. Castelletto V, Ryumin P, Cramer R, Hamley IW, Taylor M, Allsop D, Reza M, Ruokolainen J, Arnold T, Hermida-Merino D, et al: Self-Assembly and Anti-Amyloid Cytotoxicity Activity of Amyloid beta Peptide Derivatives. *Sci Rep* 2017, 7:43637.
71. Morales R, Callegari K, Soto C: Prion-like features of misfolded A β and tau aggregates. *Virus Res* 2015, 207:106-112.
72. Katzmarski N, Ziegler-Waldkirch S, Scheffler N, Witt C, Abou-Ajram C, Nuscher B, Prinz M, Haass C, Meyer-Luehmann M: A β oligomers trigger and accelerate A β seeding. *Brain Pathol* 2020, 30:36-45.
73. Bayer TA, Wirths O: Intraneuronal A β as a trigger for neuron loss: can this be translated into human pathology? *Biochem Soc Trans* 2011, 39:857-861.
74. Friedrich RP, Tepper K, Rönicke R, Soom M, Westermann M, Reymann K, Kaether C, Fändrich M: Mechanism of amyloid plaque formation suggests an intracellular basis of Abeta pathogenicity. *Proc Natl Acad Sci U S A* 2010, 107:1942-1947.
75. Gouras GK, Tampellini D, Takahashi RH, Capetillo-Zarate E: Intraneuronal beta-amyloid accumulation and synapse pathology in Alzheimer's disease. *Acta Neuropathol* 2010, 119:523-541.
76. Pensalfini A, Albay R, 3rd, Rasool S, Wu JW, Hatami A, Arai H, Margol L, Milton S, Poon WW, Corrada MM, et al: Intracellular amyloid and the neuronal origin of Alzheimer neuritic plaques. *Neurobiol Dis* 2014, 71:53-61.

Figures

Fig1

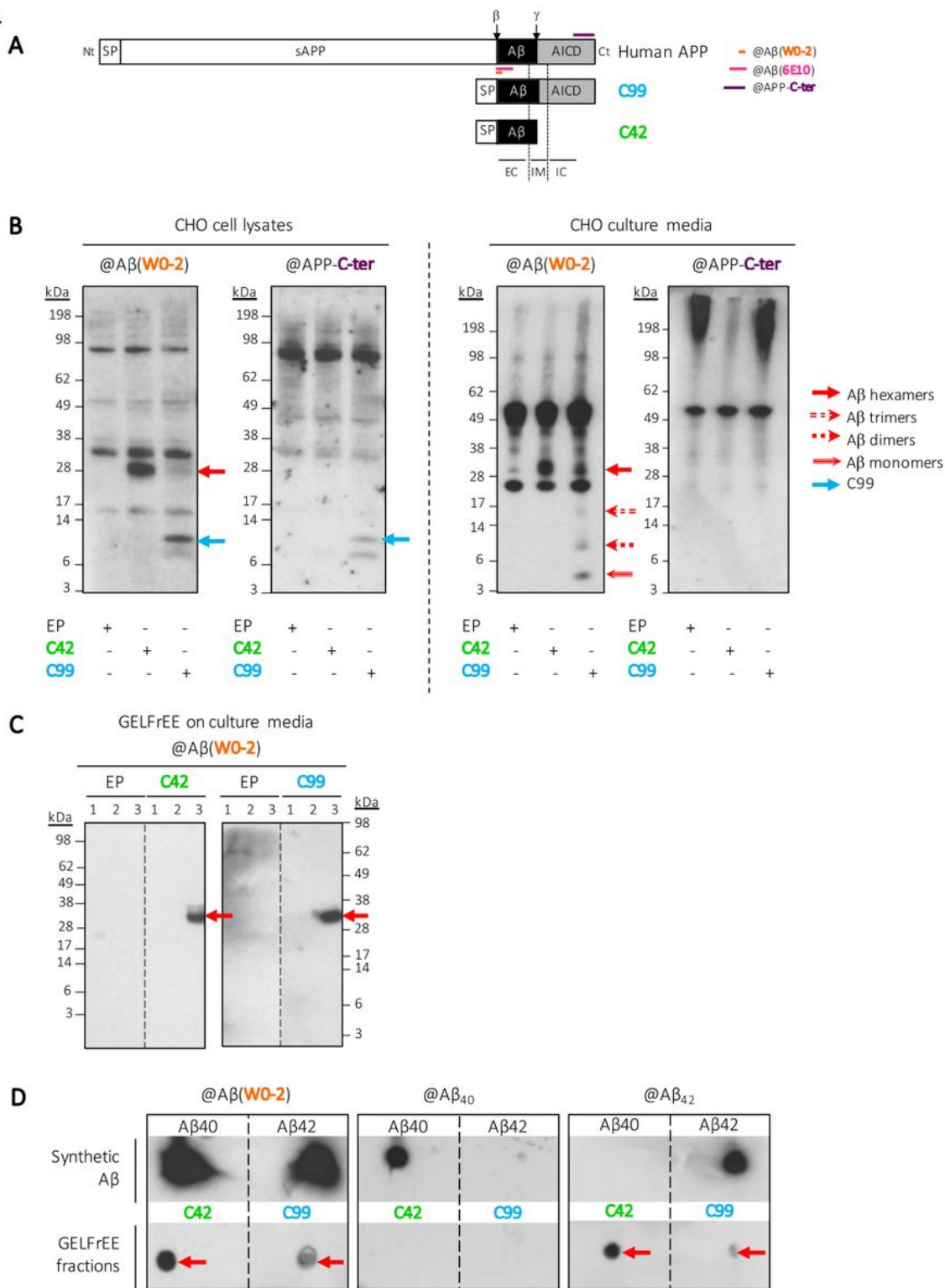


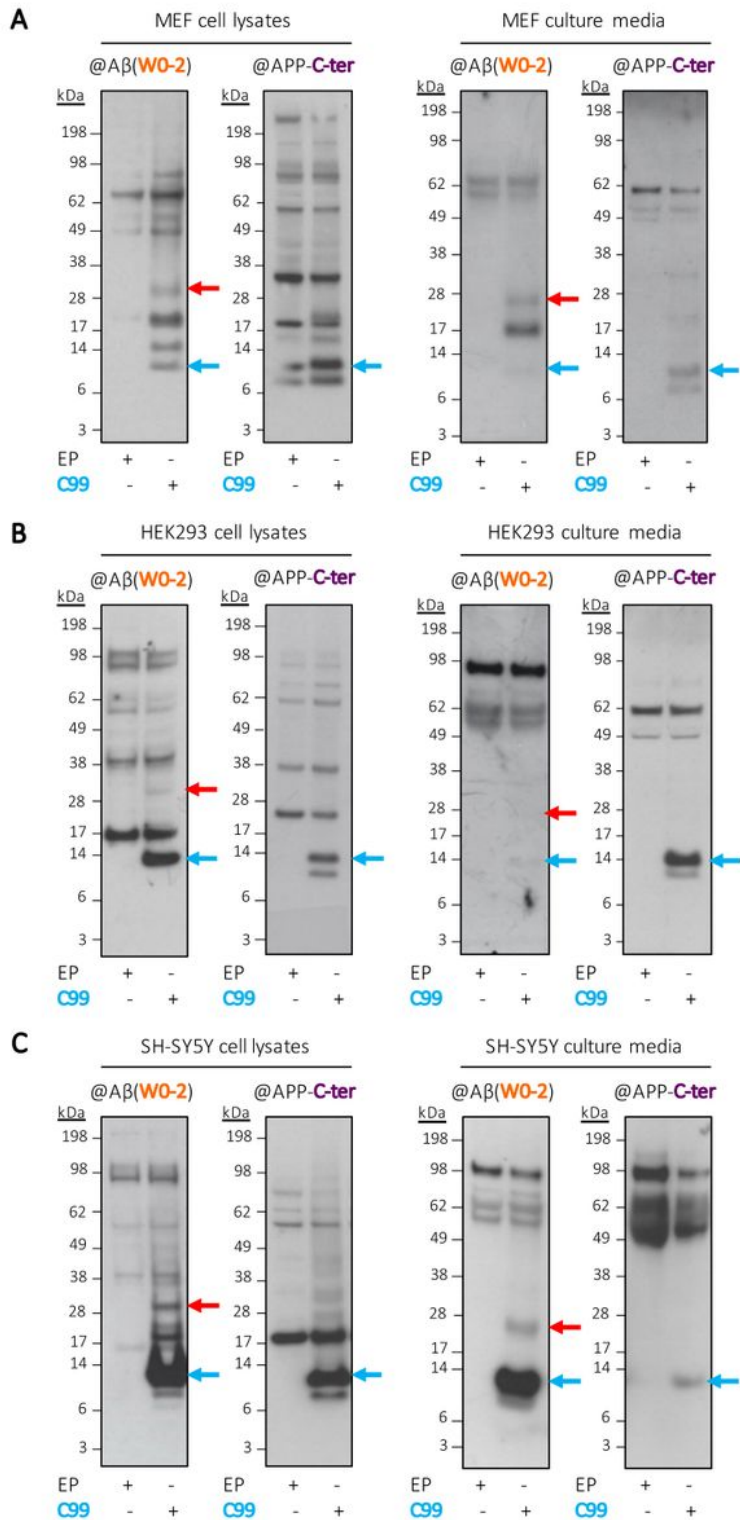
Figure 1

Detection of hexameric Aβ₄₂ in CHO cells expressing human APP metabolites. A. Full-length APP is cleaved by β-secretase at the β site, located at the N-terminus of Aβ, to produce a 99-amino acid long membrane-bound fragment called βCTF (encompassing Aβ and AICD). The construct referred to as C99 here is composed of the signal peptide (SP) of APP fused to the sequence of the βCTF fragment. This fragment is then cleaved by β-secretase at the β site to release Aβ. The C42 construct is composed of the

SP of APP and the A β 42 sequence. The epitopes of the primary antibodies directed against human A β (clones W0-2 and 6E10) and the C-terminal region of APP (APP-C-ter) used in this study are indicated on the scheme. Nt=N-terminus, Ct=C-terminus, sAPP=soluble APP, AICD=APP intracellular domain, EC=extracellular, IM=intramembrane, IC=intracellular. B. Detection of an assembly of ~28kDa by Western blotting in CHO cell lysates and culture media following expression of either C42 or C99. This assembly is recognized by the W0-2 antibody, but not by the APP-C-ter, suggesting it emerges by assembly of A β . In the media of C99-expressing cells, intermediate assemblies are also observed; monomers, dimers and trimers. EP=empty plasmid. C. Isolation of cell-derived A β . The media of CHO cells expressing either EP, C42 or C99 were immunoprecipitated and separated using the GELFrEE technique. We optimized a method to collect the ~28kDa A β assembly as an isolated liquid fraction. Dashed lines indicate that proteins were run on the same gel, but lanes are not contiguous. D. Dot blotting of the isolated ~28kDa assemblies revealed they are composed of A β 42. Synthetic preparations of monomeric A β 40 and A β 42 were used as positive controls. Combined with the observed size, we identify the assemblies of interest as A β 42 hexamers. Dashed lines indicate that proteins were loaded on the same membrane, but image was readjusted.

Fig2

 A β hexamers
 C99

**Figure 2**

Commonality of hexameric A β production in several cell lines. Cell lysates and media from human neuroblastoma SH-SY5Y (in A.) and embryonic HEK293 (in B.) cells, as well as from murine MEF fibroblasts (in C.) expressing C99 all revealed the presence of a ~28kDa band recognized by the human A β specific W0-2 antibody, and not by the anti-APP-C-ter. EP= empty plasmid.

Fig3

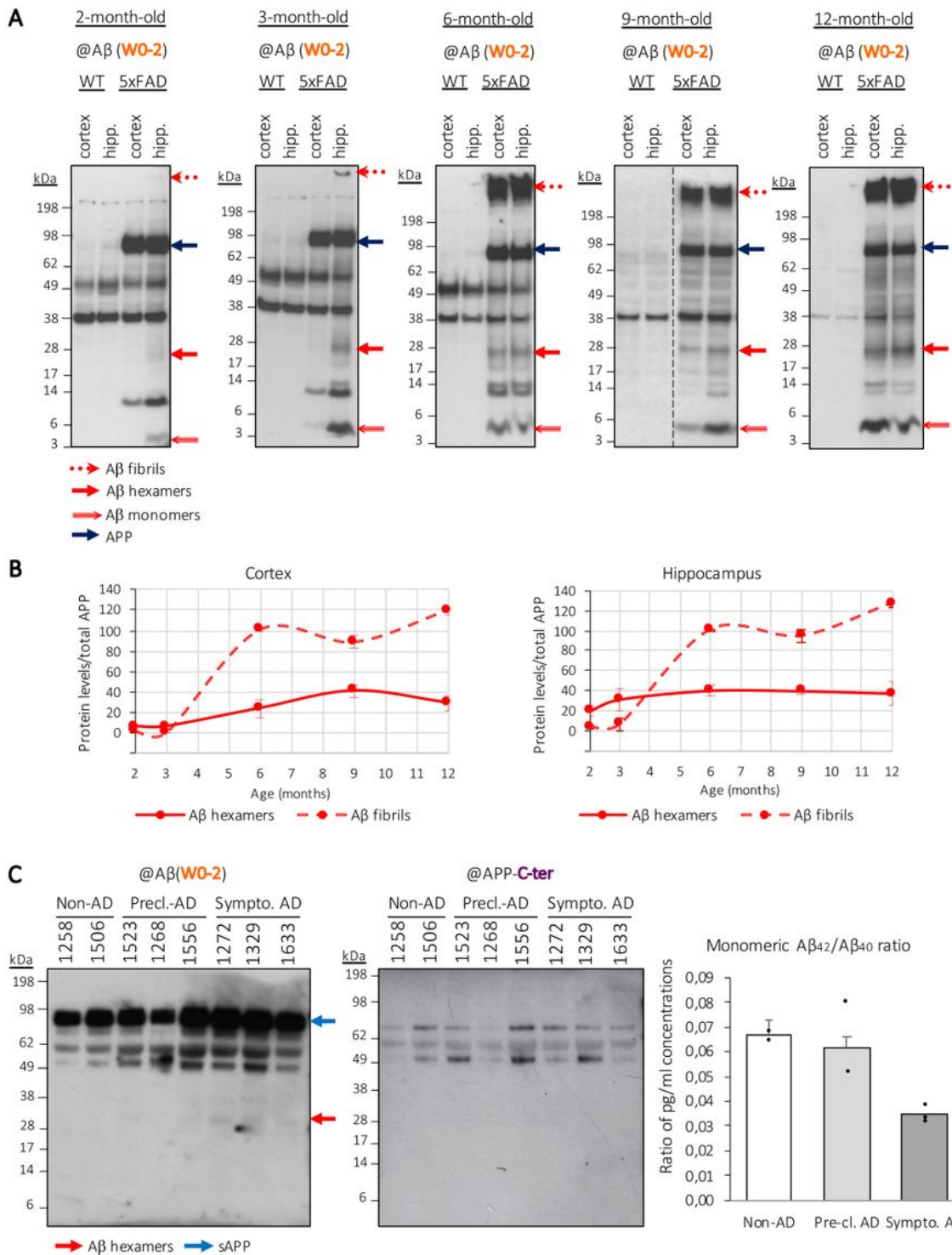


Figure 3

Identification of hexameric A β as an assembly involved in the context of AD. A. Detection of A β assemblies in brain samples from an amyloid mouse model (5xFAD). Cortices and hippocampi of euthanized mice were lysed and analyzed by Western blotting. A β fibrils appear stuck in the wells and hexameric A β assemblies are detected at ~28kDa. To note, A β monomers are also detected in all 5xFAD samples and reflect an efficient metabolism of the human APP protein expressed in these mice. Dashed

lines indicate that proteins were run on the same gel, but lanes are not contiguous. Hipp.=hippocampus. B. The signal intensities of A β hexamers and A β fibrils were quantified relatively to the APP signal. Samples used for quantitative analysis derived from the same experiment, with Western blots processed in parallel. The displayed graphs represent the profile of A β assemblies as related to both the analyzed brain area (cortex, hippocampus) and the age (2, 3, 6, 9, 12 months of age) (min N=3 each). C. Identification of hexameric A β in the cerebrospinal fluid (CSF) of cognitively affected patients. Western blotting analysis was performed using the W0-2 and APP-C-ter antibodies. Dosage of monomeric A β 42/A β 40 by ECLIA immunoassay confirmed the correct classification of individuals, with a reduction in ratio along with AD progression. sAPP=soluble APP. Pre-cl.=preclinical. Sympto.=symptomatic.

Fig4

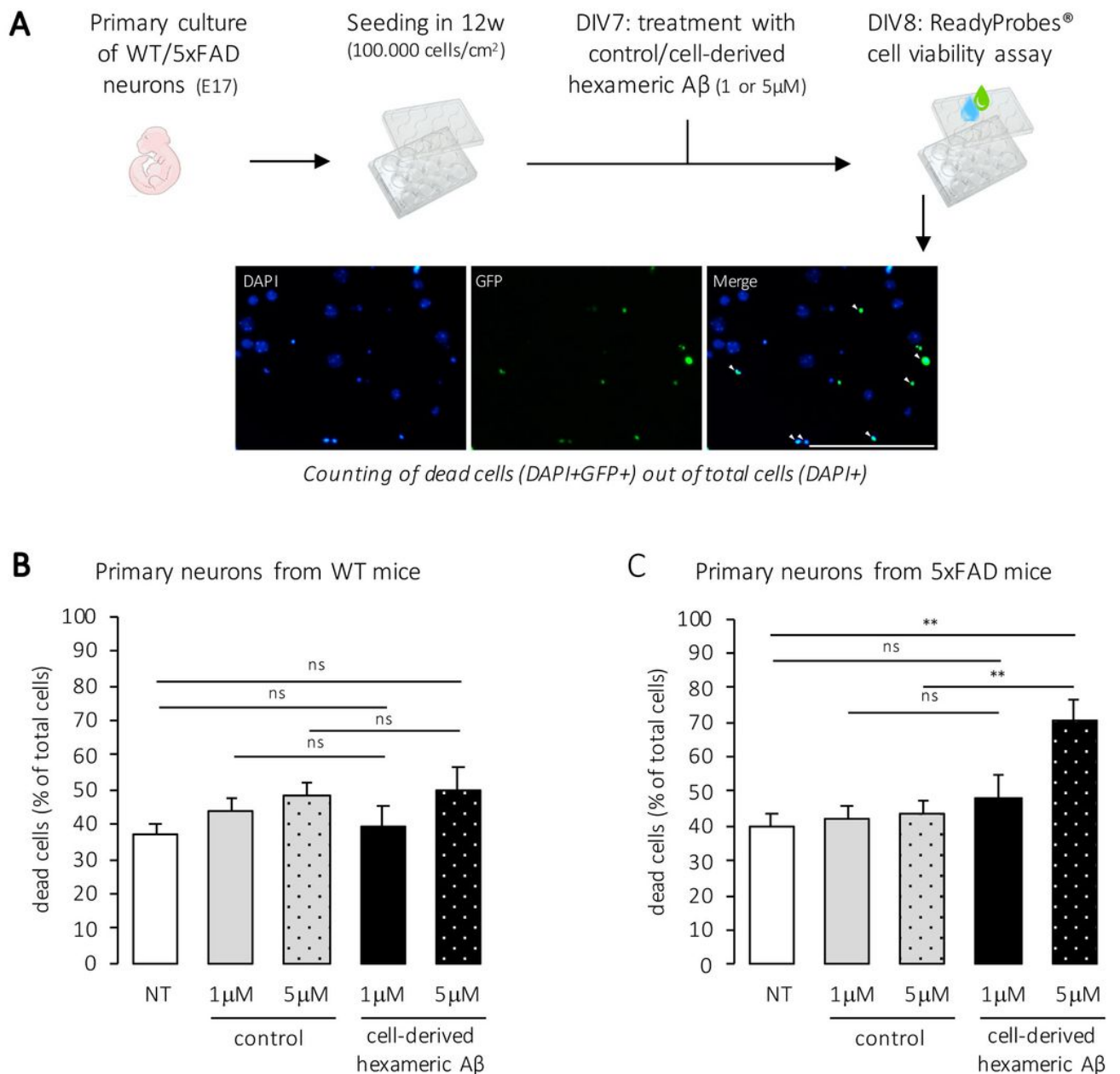


Figure 4

Cell-derived A β hexamers are only cytotoxic in primary neurons that express amyloid proteins. A. Experimental workflow. Primary neurons were isolated from wild-type (WT) or transgenic (5xFAD) mouse embryos at stage E17 and cultured for 8 days in vitro (DIV). At DIV7, cells were incubated for 24h with 1 μ M or 5 μ M of cell-derived hexameric A β or control, isolated from the media of C42- and EP-expressing CHO cells respectively. Cell viability was assessed using the ReadyProbes® assay and fluorescent staining was captured at an EVOS® FL Auto fluorescence microscope. A representative image of the assay is shown. Scale bar=50 μ m. B, C. Quantification of the proportion of dead cells compared to the total cells in WT (in B.) and 5xFAD cultures (in C.). Total number of cells counted (number of dead cells counted in brackets) was as follows in WT: n=1183(439), 1070(472), 650(314), 813(318), 797(400) and 5xFAD: n=528(212), 640(270), 1019(442), 465(224), 775(544) for NT, control (equivalent of 1 μ M), control (equivalent of 5 μ M), hexameric A β (1 μ M) and hexameric A β (5 μ M) respectively. NT=not treated. N=4 independent experiments in WT, N=3 independent experiments in 5xFAD. One-way ANOVA with Tukey's multiple comparison test: ns=non-significant, *=p<0.05, **=p<0.01 (in WT: p=0.99 NT vs hexameric A β (1 μ M), p=0.38 NT vs hexameric A β (5 μ M), p=0.95 control (1 μ M) vs hexameric A β (1 μ M), p=0.97 control (5 μ M) vs hexameric A β (5 μ M); in 5xFAD: p=0.70 NT vs hexameric A β (1 μ M), p=0.004 NT vs hexameric A β (5 μ M), p=0.85 control (1 μ M) vs hexameric A β (1 μ M) and p=0.009 control (5 μ M) vs hexameric A β (5 μ M)).

Fig5

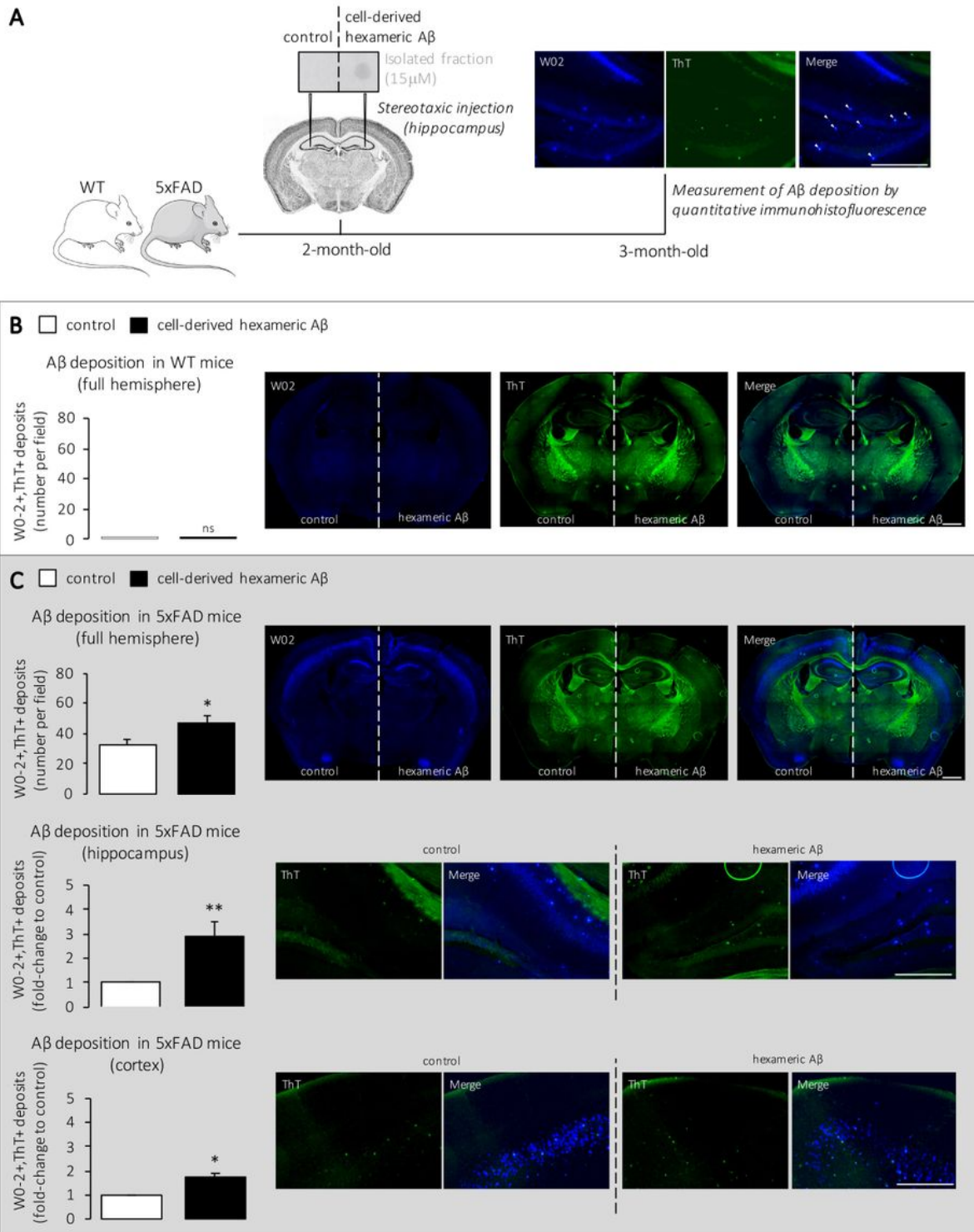
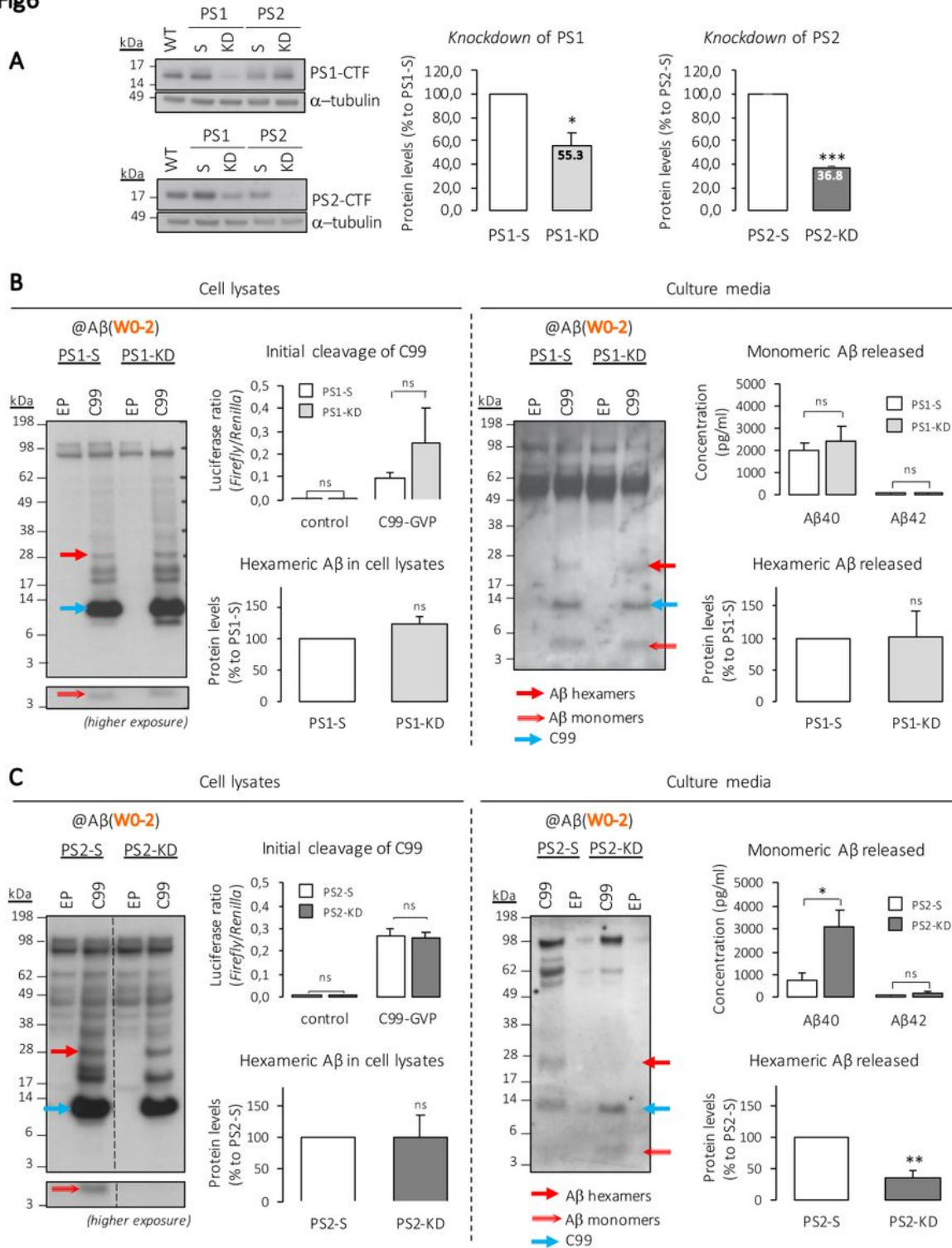


Figure 5

Intracerebral injection of cell-derived hexameric A β in WT and 5xFAD mice. A. Experimental workflow. 2-month-old mice were deeply anesthetized, placed in a stereotaxic apparatus and bilaterally injected with 2 μ l of either 15 μ M GELFrEE-isolated A β hexamers (C42) or control (EP) in the hippocampus (A/P -1.94; L +2.17; D/V -1.96; mm relative to bregma). Both fractions were analyzed by dot blotting prior to injection. 30 days later, mice were transcardially perfused, brains were fixed and coronally sectioned (50 μ m).

Immunostaining was performed on free-floating sections using the anti-human A β (W0-2) antibody as a marker for A β and the Thioflavin T (ThT) dye as a marker for fibrillar deposits. W0-2 and ThT staining were detected with FITC/Cy5 and GFP filters respectively. Right panel displays an example of double-positive counting. Scale bar=400 μ m. B, C. Quantification of fibrillar deposits in full hemispheres of WT (in B.) and 5xFAD brains (in C. upper panel) injected with control vs hexameric A β . Scale bar=1000 μ m. n=32 slides from N=8 mice for both WT and 5xFAD. Mann-Whitney test: ns=non-significant, *=p<0.05 (in WT: p>0.99 control vs hexameric A β ; in 5xFAD: p=0.04 control vs hexameric A β). For transgenic mice, deposits were also classified according to the two most affected brain regions, hippocampus and cortex, as a function of the control-injected hemisphere (in C. middle and lower panel, scale bar=400 μ m). A 2.90-fold and a 1.74-fold increase were observed in the hippocampus and cortex respectively. One-sample Wilcoxon signed-rank test with hypothetical value set at 1: *=p<0.05, **=p<0.01 (in 5xFAD hippocampus: p=0.008 control vs hexameric A β ; in 5xFAD cortex: p=0.02 control vs hexameric A β).

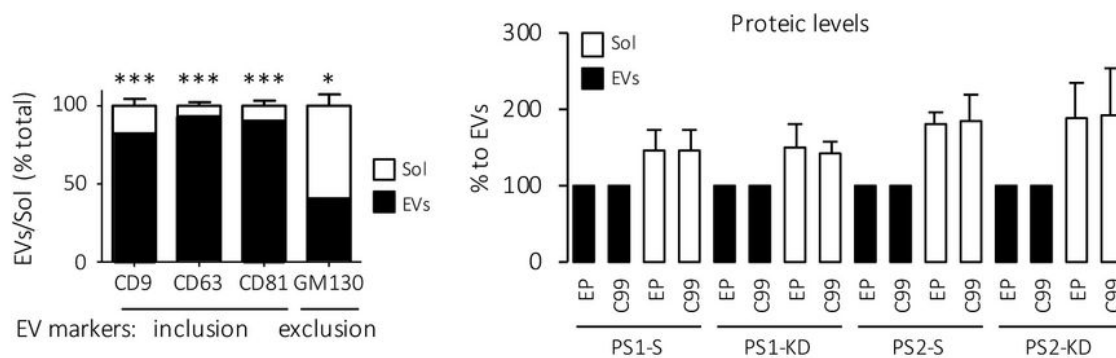
Fig6**Figure 6**

Contribution of presenilins to the production of hexameric Aβ. A. SH-SY5Y knockdown (KD) cell lines were generated using CRISPR-Cas9, with guide RNA vectors targeting either human PSEN1 (PS1-KD) or PSEN2 (PS2-KD) genes. Control cells were transfected with respective scrambled sequences. Left, a representative Western blot; middle and right, quantitative decrease in PS1 and PS2 protein levels in KD compared to S cells. N=3. One-sample t test with hypothetical value set as 100: *= $p < 0.05$, ***= $p < 0.001$ (S

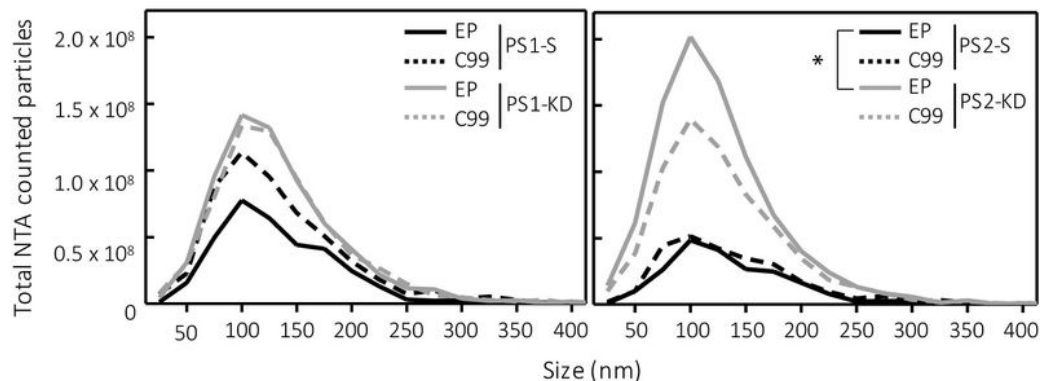
vs KD, in PS1: $p=0.03$; in PS2: $p=0.0001$). WT=wild-type, S=scramble. B, C. Initial cleavage ability was monitored by a reporter gene assay. The release of APP intracellular domain (AICD) from a tagged C99-GVP substrate was measured by the Gal4-Firefly reporter gene. Results are represented as Firefly/Renilla luciferases ratios, with Renilla serving as a transfection-efficiency control. The profile of A β production was assessed after transfection with either an empty plasmid (EP) or C99, using Western blotting and ECLIA immunoassay, in PS1-KD vs PS1-S (in B.) and in PS2-KD vs PS2-S (in C.). Dashed line indicates that proteins were run on the same gel, but lanes are not contiguous. Luciferase assays (initial cleavage of C99): N=4 each. One-way ANOVA with Tukey's multiple comparison test: ns=non-significant (S vs KD, in PS1 control: $p>0.99$; in PS1 C99-GVP: $p=0.10$; in PS2 control: $p=0.99$; in PS2 C99-GVP: $p=0.99$). Western blots quantitative analyses (hexameric A β , in cell lysates and released, relative to C99 and expressed as a % to S): N=3 each. One-sample t test with hypothetical value set as 1: ns=non-significant, **= $p<0.01$ (S vs KD, in PS1 cell lysates: $p=0.16$; in PS1 media: $p=0.97$; in PS2 cell lysates: $p=0.99$; in PS2 media: $p=0.01$). ECLIA assays (monomeric A β released): N=5 each. Mann-Whitney test: ns=non-significant, *= $p<0.05$ (S vs KD, in PS1 A β 40: $p>0.99$; in PS1 A β 42: $p>0.99$; in PS2 A β 40: $p=0.04$; in PS2 A β 42: $p=0.12$).

Fig7

A



B



C

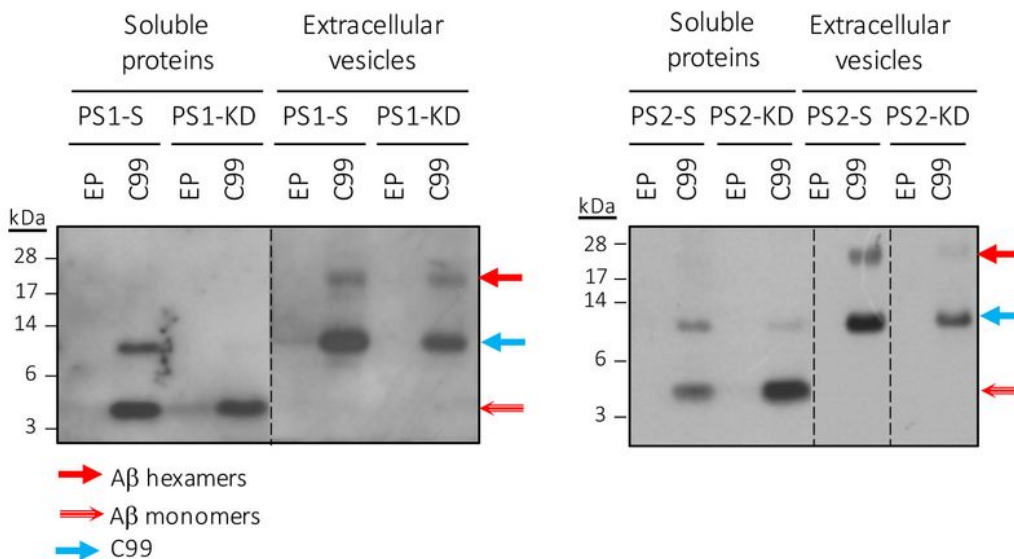


Figure 7

Localization of hexameric Aβ in extracellular vesicles (EVs). Media of PS1-S, PS1-KD, PS2-S and PS2-KD cells underwent an ultracentrifugation process to separate putative enrichment of EVs, in pellet, from soluble proteins. A. The efficiency of EVs isolation was confirmed by plate-based Europium-immunoassay (left panel) showing an enrichment of EVs inclusion markers CD9, CD63 and CD81 while EVs exclusion marker GM130 was lower in EVs as compared to soluble fractions. N=6. Mann-Whitney

test: $\ast = p < 0.05$, $\ast\ast\ast = p < 0.001$ (CD9 (n=22), CD63 (n=22) and CD81 (n=18): $p < 0.0001$; GM130 (n=19): $p = 0.0362$). Quantification of protein levels by BCA (right panel) showed larger protein amounts in soluble than EVs fractions, ruling out the specific enrichment of inclusion markers due to higher content in proteins. B. EVs ultracentrifugation pellets were counted for number of particles of 70-400nm by nanoparticle tracking analysis (NTA). n=9 in N=3 independent experiments. Two-way ANOVA with Bonferroni's multiple comparison: $\ast = p < 0.05$ (PS2-KD EP vs PS2-S EP: $p < 0.05$). C. Both EVs and soluble extracts were monitored by Western blotting with the W0-2 antibody. Dashed lines indicate that proteins were run on the same gel, but lanes are not contiguous. EP=empty plasmid, EV(s)=extracellular vesicle(s), Sol=soluble proteins fraction.

Supplementary Files

This is a list of supplementary files associated with this preprint. Click to download.

- [AdditionalFile1.pdf](#)
- [AdditionalFile2.xlsx](#)